Technical Report LSI-2012-001

An Overview of BRDF Models

Rosana Montes and Carlos Ureña

Dept. Lenguajes y Sistemas Informáticos
University of Granada, Granada, Spain
{rosana,curena}@ugr.es

Abstract

This paper is focused on the Bidirectional Reflectance Distribution Function (BRDF) in the context of algorithms for computational production of realistic synthetic images. We provide a review of most relevant analytical BRDF models proposed in the literature which have been used for realistic rendering. We also show different approaches used for obtaining efficient models from acquired reflectance data, and the related function fitting techniques, suitable for using that data in efficient rendering algorithms. We consider the algorithms for computation of BRDF integrals, by using Monte-Carlo based numerical integration. In this context, we review known techniques to design efficient BRDF sampling schemes for both analytical and measured BRDF models.

Categories and Subject Descriptors (according to ACM CCS): I.3.7 [Computer Graphics]: Three-Dimensional Graphics and Realism. Color, shading, shadowing, and texture. I.6.8 [Types of simulation]: Monte Carlo

1. Introduction

One of the goals in Computer Graphics is the production of synthetic images from digital object models. For some applications when photorealism is required, those images must exhibit some degree of visual realism. Here, the term *visual realism* means that human observers should notice as little difference as possible between a synthetic image and a real photograph of the real object whose digital model was used to produce the image.

This realism can be achieved by the production of a detailed model of geometry and materials in the scene. Part of the effort devoted to modeling must be focused on modeling the reflective properties of materials, as this is a key factor in visual realism. This is done by characterizing the directional distribution of reflectance of the materials using physical models. These models must be suitable for the design of efficient global illumination computation algorithms.

The characterization of reflective properties of materials can be achieved by defining the function which determines how reflected radiance is distributed in terms of the distribution of incident radiance. This function is the Bidirectional Reflectance Distribution Function (BRDF).

This paper is meant to serve as a tool for researchers and developers. We review the Computer Graphics literature related to the BRDF function, from theoretical models to practical BRDF-related aspects of implementation of rendering software.

The paper is organized as follows: in Section 2 we provide the formal definition of the BRDF, and we introduce its properties and main types. In Section 3, we include a review of main analytical BRDF models proposed in the literature. For each model we show their properties, advantages and disadvantages in terms of realism and computational efficiency. Section 4 is devoted to acquired BRDF models. In Section 5, we focus on the methodologies for BRDF sampling in the context of Monte-Carlo based numerical schemes for radiance integration. Section 6 finalizes with the conclusions.

2. Definition and properties of the BRDF function

Generation of realistic images relies on the numerical computation of approximations to the radiance function (denoted by L). The importance of L function in rendering comes from the fact that this quantity can be used to create simple and accurate models of image formation in the human visual system and in photographic cameras [Shi90]. In this section we introduce formal definitions and properties for several radiance-related functions. A valuable introduction to concepts and terminology can be found in [NRH*92]. A far more detailed introduction (from the perspective of trans-

port theory) can be found in [Gla94], while more practical approaches (specifically focused on Computer Graphics applications) can be found in [DBB06, PH10].

Radiance is influenced by the characteristics of materials with which electromagnetic radiation interacts by scattering, reflection and refraction. *Reflection* is the process by which electromagnetic flux (power), incident on a stationary surface or medium, leaves that surface or medium from the incident side without change in frequency [NRH*92]. Our subject (the BRDF) is useful as a model for reflection. In general, and unless otherwise stated, we do not take into account *subsurface scattering*, *refraction* in the material, or *participating media*. We also assume all photons have a single wavelength λ (*fluorescence* is not modelled), that reflection happens in a short interval around an instant of time t (we omit *phosphorescence*), and that light is *unpolarized*. However some BRDFs models do take into account the effect of some of these phenomena on the BRDF expression, and this review gives further details in those particular cases.

In general, parameters t, x and λ are implicit in our notation, however in this section x is included explicitly for clarity. Regarding λ, we exclude it from the notation for most BRDF models, except for the cases when the BRDF function depends on it.

When radiant power hits a smooth and locally planar interface between two media with different refraction indexes (*the index of refraction* of a medium is a value inversely proportional to light speed in that medium), a part of the incoming flux is reflected back to the incident medium and part is transmitted through the other medium (this part undergoes refraction, that is, a change in the orientation of the wavefront, governed by *Law of refraction* or *Snell's law*). Well known *Fresnel equations* characterize the fraction of power which is reflected and transmitted, as a function of power, direction and *polarization state* of incident light [Hec02] (the term *polarization state* is related to the evolution in time of electric and magnetic fields vibration directions).

We will use a simplified particle model for radiation, a model in which photons leaving (or reaching) x can be assigned a direction $\mathbf{u}$ (a unit-length direction vector, with $\mathbf{u} \in \Omega_x$, that is, it holds $\mathbf{u} \cdot \mathbf{n}_x \geq 0$, where $\mathbf{n}_x$ is the unit-length vector perpendicular to the surface tangent plane at x). The reflection process causes reflected photons leaving x to be distributed in arbitrary outgoing directions. The distribution of directions for these photons depends on two factors: (a) the characteristics of the material at x and (b) the distribution of directions for incoming photons at x. The BRDF depends only on the characteristics of the material. Note that Ω_x has an associated solid angle measure, which we will denote as σ. We will also use σ_p to denote projected solid angle measure, that is, σ_p is the measure on Ω_x satisfying $d\sigma_p(\mathbf{u}) := (\mathbf{u} \cdot \mathbf{n}_x)\, d\sigma(\mathbf{u})$, for any $\mathbf{u} \in \Omega_x$.

We can measure the total radiant power reaching a small area around point x per unit of time and per unit of area. This quantity is called the *irradiance* at x, written as $E(x)$, its units are $W \cdot m^{-2}$. We may restrict this measure to the total summed power of all photons coming only from directions in any given hemisphere region $R_i \subseteq \Omega_x$. We will write this as $\Phi_i(x \leftarrow R_i)$. Symbol Φ_i, thus, stands for a measure in Ω_x. Total incident power $\Phi_i(x \leftarrow R_i)$ may cause a part of it to produce reflected photons (from x) in arbitrary directions. It is possible to consider which part of it is reflected to outgoing directions in another region $R_o \subseteq \Omega_x$. We will write this power as $F_r(x, R_o \leftarrow R_i)$. Functions Φ_i and F_r have the same units as E, and both can be considered as *measure functions* (in Ω_x and $\Omega_x \times \Omega_x$, respectively). A detailed introduction to radiometric functions by using measure theory can be found in [Arv95a].

Both Φ_i and F_r are *absolutely continuous* with respect to σ_p measure. This is because for any $R_i, R_o \subseteq \Omega_x$, if $\sigma_p(R_i) = 0$ then necessarily $\Phi_i(x \leftarrow R_i) = 0$, and if either $\sigma_p(R_i) = 0$ or $\sigma_p(R_o) = 0$ then $F_r(x, R_o \leftarrow R_i) = 0$. This continuity allows to use the Radon-Nikodym derivative (twice, one for each argument of F_r) to define two new functions F_r' and F_r'' as follows:

$$F_r'(x, R_o \leftarrow R_i) := \frac{dF_r}{d\sigma_p}(x, R_o \leftarrow R_i) \tag{1}$$

$$F_r''(x, \mathbf{w}_o \leftarrow R_i) := \frac{dF_r'}{d\sigma_p}(x, \mathbf{w}_o \leftarrow R_i) \tag{2}$$

Function F_r' can be viewed as a measure function on its second argument R_i (it is the reflected power density in direction $\mathbf{w}_o$ due to power incident from region R_i). Note that F_r'' is the differential amount of power reflected at x to direction $\mathbf{w}_o$ due to reflection caused by a differential amount of power incident at x from direction $\mathbf{w}_i$. Its units are $Watt \cdot meter^{-2} \cdot steradian^{-2}$.

Two additional functions L_i and L_r can be defined by using Φ_i and F_r':

$$L_i(x \leftarrow \mathbf{w}_i) := \frac{d\Phi_i}{d\sigma_p}(x \leftarrow \mathbf{w}_i) \tag{3}$$

$$L_r(x \rightarrow \mathbf{w}_o) := F_r'(x, \mathbf{w}_o \leftarrow \Omega_x) \tag{4}$$

function L_i is the density of power arriving at x from $\mathbf{w}_i$, and is called *incident radiance*. Function L_r is the density of power reflected from x to direction $\mathbf{w}_o$, and is called *reflected radiance*. Both quantities have units for $W \cdot m^{-2} \cdot steradian^{-1}$.

The *Bidirectional Reflectance Distribution Function* (BRDF), denoted by f_r, is a function of two vectors $\mathbf{w}_i, \mathbf{w}_o \in \Omega_x$, and can be defined formally as:

$$f_r(x, \mathbf{w}_o \leftarrow \mathbf{w}_i) := \frac{F_r''(x, \mathbf{w}_o \leftarrow \mathbf{w}_i)}{L_i(x \leftarrow \mathbf{w}_i)} \tag{5}$$

this implies that we can view f_r as the amount of reflected radiance at $\mathbf{w}_o$ due to a unit of irradiance at $\mathbf{w}_i$. Its units are $steradian^{-1}$. As a ratio of two non-negative power densities, f_r is also non-negative and unbounded (although its integral is, see below). An important property is that the BRDF is

independent of L_i (the distribution of incident radiance), and only depends on the characteristics of the material around surface point x.

By using (2) and (5) it is possible to expand F'_r in (4) and express reflected radiance as a weighted integral sum of incident radiance, where the BRDF act as the weighting function:

$$\begin{aligned} L_r(x \to \mathbf{w}_o) &:= F'_r(x, \mathbf{w}_o \leftarrow \Omega_x) \\ &= \int_{\Omega_x} dF'_r(x, \mathbf{w}_o \leftarrow \mathbf{w}_i) \\ &= \int_{\Omega_x} F''_r(x, \mathbf{w}_o \leftarrow \mathbf{w}_i)\, d\sigma_p(\mathbf{w}_i) \\ &= \int_{\Omega_x} f_r(x, \mathbf{w}_o \leftarrow \mathbf{w}_i)\, L_i(x \leftarrow \mathbf{w}_i)\, d\sigma_p(\mathbf{w}_i) \end{aligned} \tag{6}$$

The *albedo* (also called *Bi-hemispherical reflectance*) at point x is the ratio of total outgoing power to total incident power. It is written as $\rho(x)$ (or simply ρ) and can be defined as:

$$\rho(x) := \frac{F_r(x, \Omega_x \leftarrow \Omega_x)}{\Phi_i(x \leftarrow \Omega_x)} \tag{7}$$

Sometimes it is useful to consider the amount of total reflected power in all directions due a unit of power coming from a single incident direction[†] $\mathbf{w}_i$. This is the *directional-hemispherical* reflectance, ρ_{dh}, and can be defined as follows:

$$\rho_{dh}(x \leftarrow \mathbf{w}_i) := \int_{\Omega_x} f_r(x, \mathbf{w}_o \leftarrow \mathbf{w}_i)\, d\sigma_p(\mathbf{w}_o) \tag{8}$$

Note that both albedo and directional-hemispherical reflectance depend only on the BRDF at x.

In this paper, we consider each particular BRDF function as a formal model for a particular distribution of reflected radiance which happens in nature. This kind of models is usually called *physically plausible BRDFs*, in contrast with *non-physical BRDF* models, which cannot exist in nature but can be used for applications where it is not necessary or desirable to reproduce natural reflection. As stated, a physically plausible BRDF must be non-negative, but it also must obey these two additional properties:

Symmetry: The *Helmholtz Reciprocity Rule* [Hel25] states that the BRDF is symmetric, that is:

$$\forall\, \mathbf{u}, \mathbf{v} \in \Omega_x \;:\quad f_r(x, \mathbf{u} \leftarrow \mathbf{v}) \;=\; f_r(x, \mathbf{v} \leftarrow \mathbf{u})$$

this symmetry property leads us to use a notation where a double arrow is written between both vectors, thus we will write $f_r(x, \mathbf{w}_o \leftrightarrow \mathbf{w}_i)$ instead of $f_r(x, \mathbf{w}_o \leftarrow \mathbf{w}_i)$. It is important to state that this property does not hold always but just for certain polarization states of light [Hel25], [CP85]. However, in computer graphics and computer vision literature, BRDF models are usually assumed to obey this property, although some researchers have explored the consequences of non-symmetric BRDFs in the implementation of rendering systems [Vea97].

Energy Conservation: Energy conservation implies that no more radiant energy can be reflected from a point than the energy incident to that point, that is $\rho(x) \leq 1$. Moreover, as this is true for any L_i, it is in particular true for a L_i in which all the energy comes from a single direction $\mathbf{w}_i$, and this implies that $\rho_{dh}(x \leftarrow \mathbf{w}_i) \leq 1$. From this and (8) we get the following inequality:

$$\forall\, \mathbf{v} \in \Omega_x \;:\quad \int_{\mathbf{u} \in \Omega_x} f_r(x, \mathbf{u} \leftrightarrow \mathbf{v})\, d\sigma_p(\mathbf{u}) \;\leq\; 1$$

due to symmetry, this is also true if we integrate on the second variable instead. Many BRDF models include in their formulation a normalization factor —different for each one— necessary to correctly bound the resulting albedo.

A BRDF is *plausible* if it is non-negative, energy conservative and reciprocal. BRDF functions can be categorized in two classes according to the presence (or absence) of rotational symmetry. Let us use the symbol Rot_α to denote a rotation transformation of α radians (with $\mathbf{n}_x$ as axis) for vectors in Ω_x. A material is called *isotropic* if $f_r(x, Rot_\alpha \mathbf{w}_o \leftrightarrow Rot_\alpha \mathbf{w}_i)$ is independent of α, and *anisotropic* when that does not hold.

Total radiance $L(x \to \mathbf{w}_o)$ leaving x in direction $\mathbf{w}_o$ is defined as the sum of *emitted radiance* $L_e(x \to \mathbf{w}_o)$ (radiation produced in the material not due to reflection) and reflected radiance $L_r(x \to \mathbf{w}_o)$. Moreover, incoming radiance at x from $\mathbf{w}_i$ is equal to the outgoing radiance from another point y on the reverse direction (that is, $L_i(x \leftarrow \mathbf{w}_i) = L(y \to -\mathbf{w}_i)$), because in empty space radiance is conserved along straight lines. Thus, by using (6), the value of the radiance function L at vacum can be written as:

$$\begin{aligned} L(x \to \mathbf{w}_o) &= L_e(x \to \mathbf{w}_o) \\ &\quad + \int_{\Omega_x} f_r(x, \mathbf{w}_o \leftrightarrow \mathbf{w}_i)\, L(y \to -\mathbf{w}_i)\, d\sigma_p(\mathbf{w}_i) \end{aligned} \tag{9}$$

This equation expresses radiance at one point as a weighted integral sum of radiance from other points in the scene and is called the *rendering equation*. It is an example of a variant of a Fredholm-type integral equation of the second kind, with f_r as the kernel and L being the unknown function. It can be proved that a solution exists and it is unique, provided f_r obeys conservation of energy (see [ATS94], section 5.3, note that ρ_{dh} must be strictly less than one).

As has been stated, the main goal in Global Illumination is computation of values of the radiance function L. However, this is a complex calculation because in Eq. (9) function L appears on both sides, that is, it can be interpreted as a *recursive* definition of L. Radiance is usually computed in Global Illumination by using Finite Elements methods and Monte Carlo (MC) integration techniques, because it is often impossible to obtain analytic expressions for L [DBB06]. When using Monte-Carlo algorithms for rendering, an important step is *BRDF sampling*, which is described in more detail in section 5 of this paper.

[†] L_i is an ideal Dirac-delta, zero everywhere except for $\mathbf{w}_i$.

2.1. BRDF parametrization

In this section we introduce several alternative BRDF parameters domains or *parametrizations*. Original BRDF definition in (5) clearly implies that the domain is $\Omega_x \times \Omega_x$. However each BRDF model can be expressed by using different formulae depending on how vectors in Ω_x are represented. This leads to different formulae complexity, and different accuracy when fitting data based on measurements. Moreover, it yields also different time complexity and numerical accuracy in BRDF-related computations.

Parametrizations make use of various particular direction vectors in Ω_x, which we introduce here:

- *Tangent vector* ($\mathbf{t}$), this vector is perpendicular to $\mathbf{n}_x$ and thus tangent to the surface at x. It is used to build a local reference system. BRDF expressions can be refered to. Isotropic BRDFs may use any tangent vector, however for anisotropic BRDFs this vector must be considered as an external parameter which fixes the orientation of the BRDF (with respect to rotations around $\mathbf{n}_x$).
- *Bitangent vector* ($\mathbf{b}$), defined as $\mathbf{b} := \mathbf{n}_x \times \mathbf{t}$.
- *Halfway vector* ($\mathbf{h}$), defined as $\mathbf{h} := (\mathbf{w}_i + \mathbf{w}_o)/\|\mathbf{w}_i + \mathbf{w}_o\|$
- Vector $\mathbf{b}'$, defined as $\mathbf{n}_x \times \mathbf{h}/\|\mathbf{n}_x \times \mathbf{h}\|$. In the case $\mathbf{n}_x = \mathbf{h}$, vector $\mathbf{b}'$ is defined equal to $\mathbf{b}$.
- Vector $\mathbf{t}'$, defined as $\mathbf{b}' \times \mathbf{h}$

Parametrizations are usually referred to local reference frames. By using the vectors introduced above, we can define reference frame Ref_n, whose X,Y and Z axes are aligned with $\mathbf{t}$, $\mathbf{b}$ and $\mathbf{n}_x$, respectively. We can also define reference frame Ref_h, whose Z axis is aligned with the halfway vector $\mathbf{h}$, Y axis is aligned with $\mathbf{b}'$, and X axis is aligned with $\mathbf{t}'$. These reference frames allow us to define various possible parameters domains in Ω_x.

Global cartesian coordinates: in these cases, vectors $\mathbf{w}_i$ and $\mathbf{w}_o$ are expressed as 3-tuples containing world coordinates, that is, coordinates relative to world reference system used to express objects geometry in the scene model.

Local cartesian coordinates: now, $\mathbf{w}_i = (x_i, y_i, z_i)$ and $\mathbf{w}_o = (x_o, y_o, z_o)$ are again expressed as 3-tuple, however these tuples contain coordinates relative to local reference frame Ref_n. Thus, the following equalities hold:

$$\begin{array}{lll} x_i := \mathbf{w}_i \cdot \mathbf{t} & y_i := \mathbf{w}_i \cdot \mathbf{b} & z_i := \mathbf{w}_i \cdot \mathbf{n}_x \\ x_o := \mathbf{w}_o \cdot \mathbf{t} & y_o := \mathbf{w}_o \cdot \mathbf{b} & z_o := \mathbf{w}_o \cdot \mathbf{n}_x \end{array} \quad (10)$$

Spherical coordinates: in this case, vectors are expressed as 2-tuples: $\mathbf{w}_i = (\varphi_i, \theta_i)$ and $\mathbf{w}_o = (\varphi_o, \theta_o)$. Each pair contains the *azimuthal angle* and *normal angle*, respectively (see Figure 2.1, left). These angles can be defined from local coordinates (as defined in (10)), as follows:

$$\begin{array}{ll} \varphi_i := atan2(y_i/x_i) & \theta_i := \arccos(z_i) \\ \varphi_o := atan2(y_o/x_o) & \theta_o := \arccos(z_o) \end{array} \quad (11)$$

Spherical coordinates for isotropic BRDFs: these BRDFs depend only on the difference between φ_i and φ_o, but not on the two individual values. Thus it is possible to express the BRDF just in terms of three values, namely θ_i,θ_o and φ_Δ, where $\varphi_\Delta := \varphi_o - \varphi_i$

Half angle- difference parametrization: this parametrization was introduced by Rusinkiewicz [Rus98], who showed it is well suited for functional approximation of reflectance data based on measurements (see section 4.2). The BRDF is expressed in terms of the spherical coordinates of $\mathbf{h}$ relative to Ref_n, which are written as (φ_h, θ_h), and the spherical coordinates of $\mathbf{w}_i$ relative to Ref_h, written as (φ_d, θ_d) respectively (see Figure 2.1, right). Thus, these angles can be defined as:

$$\begin{array}{ll} \varphi_h := atan2(y_h/x_h) & \theta_h := \arccos(z_h) \\ \varphi_d := atan2(y_d/x_d) & \theta_d := \arccos(z_d) \end{array} \quad (12)$$

where:

$$\begin{array}{lll} x_h := \mathbf{h} \cdot \mathbf{t} & y_h := \mathbf{h} \cdot \mathbf{b} & z_h := \mathbf{h} \cdot \mathbf{n}_x \\ x_d := \mathbf{w}_i \cdot \mathbf{t}' & y_d := \mathbf{w}_i \cdot \mathbf{b}' & z_d := \mathbf{w}_i \cdot \mathbf{h} \end{array} \quad (13)$$

Note that isotropic BRDFs are independent of φ_h, thus these BRDFs can be expressed just in terms of θ_h,θ_d and φ_d.

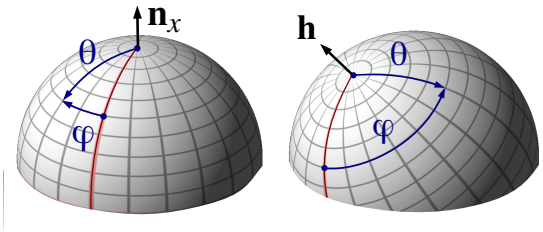

Figure 1: *Spherical coordinates, including azimuthal angle (φ), and elevation angle (θ), for vectors in Ω_x. Coordinates can be relative to the reference system Ref_n, with Z axis aligned with $\mathbf{n}_x$ (left) or relative to reference system Ref_h, with Z aligned with $\mathbf{h}$ (right). Red arc includes vectors with $\varphi = 0$.*

2.2. General classification

In general BRDF models can be classified into one or two of these categories: empirical, theoretical and experimental. Moreover, a BRDF can be based on a previous one, extending their capabilities and the type of material that it is able to model. Figure 2 represents a graphical classification of the BRDFs which are introduced in section 3.

Empirical
Their main aim is to provide a simple formulation specifically designed to mimic a kind of reflection. Consequently, we get a fast computational model adjustable by parameters, but without considering the physics behind it.

Theoretical
These models try to accurately simulate light scattering by using physics laws. They usually lead to complex expression and high computational effort, thus they are not normally employed in rendering systems.

Experimental
The BRDF can be acquired using a gonioreflectometer [War92, GA97, GA99, HLW06] which mechanically varies light source and sensor positions. This process could take hours and usually data is limited by some

angular resolution. Other techniques use digital cameras to acquire many BRDF samples with a single photograph [DGNK99, MPBM03]. No much densely acquired data is readily available.

We have the power of using the reflectance data directly in the rendering process as [MPBM03] obtaining great realism in the visual results. The other option is to approximate the reflectance data with an analytical expression. We get a formula which is simple, fast, accurate and adjustable by parameters. Some reflectance models (empirical or theoretical) are being designed for this use in mind. In these cases the parameters are not necessarily intuitive as they are meant to be set algorithmically to fit measurement data. Additionally the fitting of data presents several problems [KC08]: (1) the measurement error introduced in data could make it difficult to find a better fit for your model, (2) the solution to the fitting process (global minimum) is not guaranteed, (3) is not easy to know what is the best objective function, and what are the initial values to use, and (4) in some cases, you need to find a suitable number of lobes (it is recommended three or four in the Lafortune BRDF [NDM05]), at the expense of the non-linear minimizer becomes unstable and fails to find the minimum objective function.

3. A review of BRDF models

In this section we make a review of some of the models proposed in the literature, following the classification suggested in Figure 2. We introduce the desirable properties for BRDF models, and then we analyze if a particular model fulfill them and in what degree. Table 1 summarizes some of characteristics of the reflectance models reviewed in this paper, including their relative computational cost considering that we have implemented 16 of them.

It is understood in Computer Graphics that reflectance models should exhibit a set of desirable properties [Shi96] to make them realistic and reliable at the same time:

1. Physically plausible: a function that obeys non-negativity, reciprocity and the law of energy conservation. A BRDF with this property can be used safely in a rendering system, avoiding situations where energy is created wrong.
2. Expressive: the model is adjustable by parameters. These should be intuitive to set.
3. Usable: capable of representing as many different materials as possible, including those acquired with a device.
4. Realistic: close to actual BRDF functions which can be found in nature, showing directional diffuse and Fresnel behaviors.
5. Efficient: must lead to efficient implementations on Global Illumination rendering algorithms and thus quick to evaluate and appropriate for importance sampling of Monte-Carlo integration.
6. Accurate: Reflection components (diffuse, directional-diffuse, specular) should be represented by the model itself, avoiding ideal simplifications.

Models	Physical	Plausible	Fresnel Eq.	Anisotrotopic	Sampling	Rel.Cost (cycles)	Material Type
Ideal Specular	★	★	▼	▼	★	x	perfect specular
Ideal Diffuse	★	★	▼	▼	★	x	perfect diffuse
Minnaert	▼	···	▼	▼	▼	$5.35x$	Moon surf.
Torrance-Sparrow	★	▼	★	★	▼	···	rough surf.
Beard-Maxwell	★	▼	★	▼	▼	$397x$	painted surf.
Blinn-Phong	▼	▼	▼	▼	★	$9.18x$	rough surf.
Cook-Torrance	★	★	★	▼	▼	$16.9x$	metal,plastic
Kajiya	★	▼	★	★	▼	···	metal,plastic
Poulin-Fournier	★	▼	▼	★	▼	$67x$	clothes
Strauss	▼	···	★	▼	▼	$14.88x$	metal,plastic
He et al.	★	★	★	▼	▼	$120x$	metal
Ward	▼	▼	▼	★	★	$7.9x$	wood
Westin	★	···	★	★	▼	···	metal
Lewis	▼	★	▼	▼	★	$10.73x$	mats
Schlick	▼	★	★	★	▼	$26.95x$	heterogeneous
Hanrahan	★	···	★	▼	▼	···	human skin
Oren-Nayar	★	★	▼	▼	★	$10.98x$	matte, dirty.
Neumann	▼	★	▼	★	★	···	metal,plastic
Lafortune	▼	★	▼	★	★	$5.43x$	rough surf.
Coupled	★	★	★	▼	★	$17.65x$	polished surf.
Ashikhmin-Shirley	★	▼	★	★	★	$79.6x$	polished surf.
Granier-Heidrich	★	···	★	▼	▼	···	old-dirty metal

Table 1: *Brief summary of the properties exhibited by the reviewed BRDFs. Legend: (★) if the BRDF has this property; (▼) if the BRDF does not; (···) unknown value.*

3.1. Physical-based Reflectance Models

Ideal Reflection

In case of ideal specular reflection, light incoming from a given direction is reflected in a single direction following the *law of reflection*. The BRDF in this case is a delta dirac distribution, $\eth$, giving always zero, except for the reflection direction $\mathbf{r}$. This reduces the radiance computation considerably since $L_r(x \rightarrow \mathbf{w}_o) = L_i(x \leftarrow \mathbf{r}_{\mathbf{w}_o})$.

$$f_r(\mathbf{w}_o, \mathbf{w}_i) \;=\; \rho_s(\mathbf{w}_i)\,\eth(\mathbf{w}_o, \mathbf{w}_i)$$

where ρ_s is the specular reflectance at the point and $\eth$ is defined as follows:

$$\eth(\mathbf{r_u}, \mathbf{v}) \stackrel{\text{def}}{=} \begin{cases} \infty & if\ \mathbf{v} = \mathbf{r_u} \\ 0 & else \end{cases}$$

For this BRDF, its hemispherical integral is 1 when the incident and the outgoing direction are at the same angle relative to the surface normal and 0 otherwise.

A diffuse surface has a BRDF that has the same value for all incident and outgoing directions. This substantially reduces the computations and thus it is commonly used to model diffuse surfaces as it is physically plausible, even though there are no pure diffuse materials in the real world. This BRDF is expressed as:

$$f_r(\mathbf{w}_o, \mathbf{w}_i) \;=\; \frac{\rho_d}{\pi}$$

where ρ_d is the diffuse reflection[‡]. It includes the value π for

[‡] The fraction of energy reflected w.r.t. the total incident energy, that is $\frac{\Phi_r(x \rightarrow R_o)}{\Phi_i(x \leftarrow R_i)}$ by using the terminology introduced in section 2.

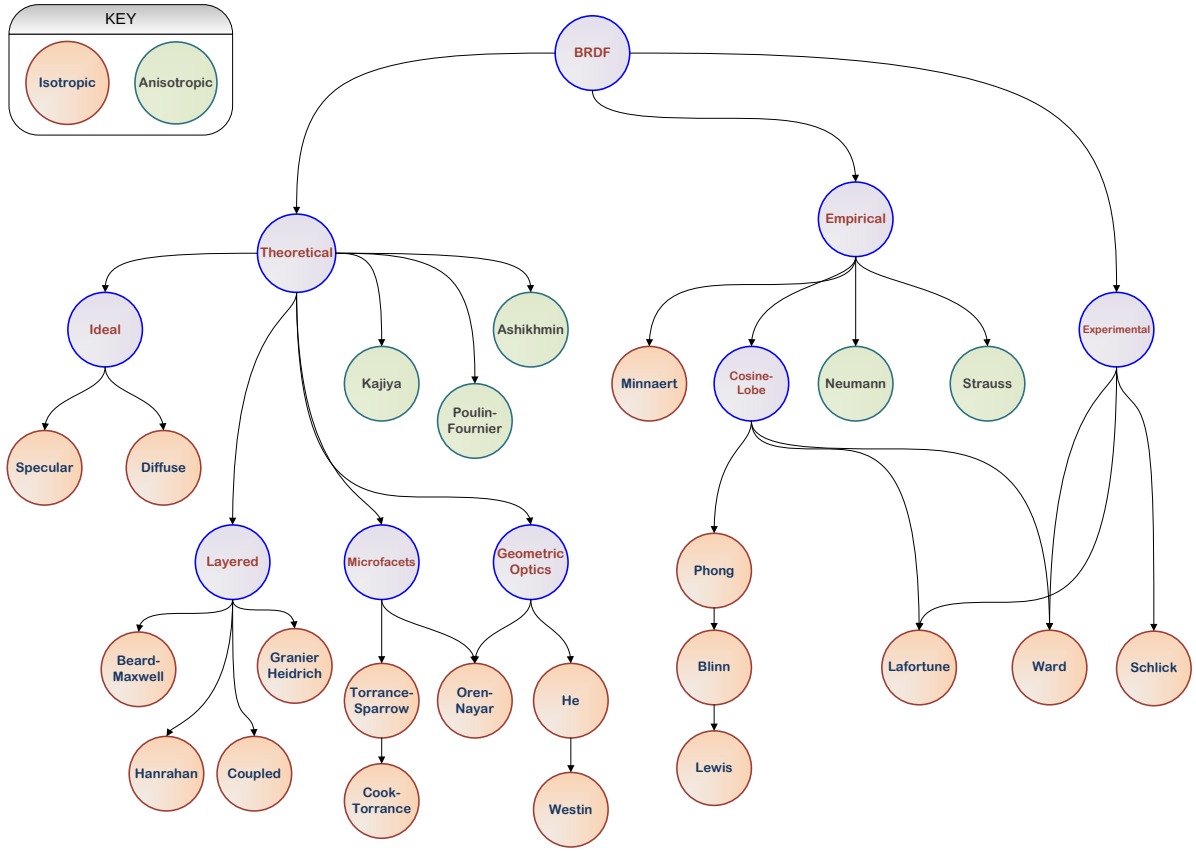

Figure 2: *A graphical classification of the BRDFs cited in this paper. Some BRDFs are built on previous ones.*

normalization, so is the result of integrate $\cos(\mathbf{v})$ in the hemisphere of directions to compute the reflectivity or albedo.

The Torrance-Sparrow BRDF

This BRDF is one of the most complete physical reflection models for isotropic materials. It is considered precursor to other models and its formulation has been validated by a ray-tracing-like simulation [MWM*98]. It considers polarized light and is used for rough surfaces [TS66, TS67]. The roughness is modelled using microscopic concavities in V-form of equal length called microfacets. Their orientation is random and their distribution is controlled by parameters, so it is possible to simulate different degrees of roughness. The complete BRDF function is as follows:

$$f_r(\mathbf{w}_o, \mathbf{w}_i) = \frac{k_d}{\pi} + \frac{k_s}{4\pi(\mathbf{n}\cdot\mathbf{w}_i)} D(\mathbf{h})\, F(\mathbf{w}_o)\, G(\mathbf{w}_o, \mathbf{w}_i)$$

We consider the previous terms separately:

- The microfacets distribution $D : \Omega \to \mathbb{R}$ with $\int_\Omega D(\mathbf{h}) = 1$ gives a distribution of the normals of the microfacets that are aligned relative to vector $\mathbf{h}$ and it is parameterized by m. Many authors use the Gaussian distribution function but the Beckmann distribution [BS63] is also common:

$$D(\mathbf{h}) = \frac{1}{m^2\cos(\delta)^4} \exp\left(\frac{\cos(\delta)^2 - 1}{m^2\cos(\delta)^2}\right)$$

- The Fresnel factor $F(\mathbf{w}_o) \in [0,1]$ gives the fraction of light that is reflected from the entire surface. Its computation is a linear combination of the coefficient for perpendicular light polarization and the coefficient for parallel light polarization. It is quite usual to use the Schlick approximation of this computation [Sch94b].
- Geometric attenuation factor $G(\mathbf{w}_o, \mathbf{w}_i) \in [0,1]$ expresses, for two directions, the ratio of light that is not occluded by the surface due to *masking* or *shadowing*. This model takes these effects into account by evaluating the following formula:

$$G(\mathbf{w}_o, \mathbf{w}_i) = \min\left\{1, \frac{2(\mathbf{n}\cdot\mathbf{h})(\mathbf{n}\cdot\mathbf{w}_o)}{(\mathbf{w}_o\cdot\mathbf{h})}, \frac{2(\mathbf{n}\cdot\mathbf{h})(\mathbf{n}\cdot\mathbf{w}_i)}{(\mathbf{w}_o\cdot\mathbf{h})}\right\}$$

This microfacet model was the basis for many other works who offered variations on the calculation of the functions D, F and G. Figure 3 shows the vector system involved in the local reflection at a given surface point, and will be referenced in subsequent reflectance models.

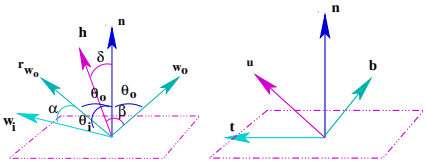

Figure 3: *Angles relative to incident and reflected vectors in a local coordinate system.*

The Beard-Maxwell BRDF

With the description of this BRDF [MBW*73] one can simulate, based on physical properties, a very concrete type of material: painted surfaces. The final model considers the combined contributions of a local specular reflection on the first layer (whose normal is $\mathbf{n}$), named $f_{r,sup}$, and a volumetric reflection approximation which comes from the reflection of light in the interior layers, simulating subsurface scattering and noted by $f_{r,vol}$.

$$f_r(x,\lambda,\mathbf{w}_o,\mathbf{w}_i) \;=\; f_{r,sup}(\lambda,\mathbf{w}_o,\mathbf{w}_i)+f_{r,vol}(\lambda,\mathbf{w}_o,\mathbf{w}_i)$$

The superficial component computes a specular reflection that takes place on the first layer of the surface. The first layer is represented by microfacets whose normals are oriented following a statistic distribution D, as the used by Torrance-Sparrow. It is also governed by the Fresnel term F for dielectrics (using $\kappa = 0$ and $\eta = 1.65$):

$$f_{r,sup}(\mathbf{w}_o,\mathbf{w}_i) \;=-\frac{F(\beta)}{F(0)}\,\frac{f_r(\mathbf{h})\cos^2(\mathbf{h})}{\cos(\mathbf{w}_o)\cos(\mathbf{w}_i)}\,SO(\mathbf{w}_o,\mathbf{h},\tau,\upsilon)$$

$$f_r(\mathbf{h}) \;=\; \frac{F(0)\,D(\mathbf{h})}{4\cos(\mathbf{w}_o)\cos(\mathbf{w}_i)}$$

As with Torrance-Sparrow [TS66, TS67], the surface is modelled with microfacets so the same *shadowing* and *masking* (here is called *obscuration*) could occur. Though the light is blocked in the same form, the formulation that models this effect is not the same. The term SO summarizes both situations, and is dependent of two parameters τ and υ that take their values from measured data:

$$SO(\mathbf{w}_o,\mathbf{h},\tau,\upsilon) \;=\; \frac{1+\frac{\theta_\mathbf{h}}{\upsilon}\,e^{-2\beta/\tau}}{1+\frac{\theta_\mathbf{h}}{\upsilon}}\left(\frac{1}{1+\frac{\phi_\mathbf{h}}{\upsilon}\,\frac{\theta_{\mathbf{w}_o}}{\upsilon}}\right)$$

The volumetric component is a simple model of the subsurface scattering of the light, where light is supposed to be depolarized:

$$f_{r,vol\,\lambda}(\mathbf{w}_o,\mathbf{w}_i) \;=\; \frac{2\,\rho_v\,f(\beta)\,g(\theta_\mathbf{h})}{\cos(\mathbf{w}_o)\cos(\mathbf{w}_i)}$$

where ρ_v is the measured reflectance of the surface when $\theta_{\mathbf{w}_o} = \theta_{\mathbf{w}_i} = 0$ and $f(\beta) = g(\theta_\mathbf{h}) = 1$ is used. For a complete description of the f and g functions please refer to the original paper [MBW*73].

Westlund and Meyer published a database of 400 measured materials which fitted with a modified Beard-Maxwell BRDF named *NEF-BM* [WM02]. This modification simplifies the original formulation by dropping the parameter $\phi_\mathbf{h}$ and the f and g functions.

The Cook-Torrance BRDF

Based on geometrical optics theory and in previous studies [BS63, TS67], Cook & Torrance developed a model that introduced new ideas: only those microfacets oriented toward $\mathbf{h}$ vector contribute to the final reflection. This model [CT82] also introduces a new type of material in the field of rendering, differentiating between metallic and non-metallic surfaces.

Reflection is described using a combination of the diffuse and specular parts with parameters k_d and k_s controlling the fraction of energy that is diffusely or specularly reflected. This parameters are considered a characteristic of the material. The diffuse term is represented by a classical Lambertian reflection. The specular term is the compound of the already known functions F, D and G of the Torrance-Sparrow model [TS67]. In this case, the normalized halfway vector simulates an imaginary surface which behaves as a mirror, and the Fresnel term represents the reflection of polished surfaces.

One of the major contributions of this work [CT82] was the development of an optimized formulation of Fresnel, making this model more applicable to Computer Graphics. In the original formulation, the energy reflected depends on the index of refraction η, and the absorption coefficient κ. For some materials both values are unknown, but could be approximated by assuming that the value of the reflectance at normal direction is constant. This facilitates to solve the coefficients dependent on the wavelength: a) η is calculated assuming that $F(\frac{\pi}{2}) = 1$ and $\kappa = 0$; b) κ is calculated by knowing $F(0)$ and having $\eta = 1$. Finally the simplified Fresnel expression is:

$$F(\theta) \;=\; \frac{1}{2}\,\frac{(b-c)^2}{(b+c)^2}\left\{1+\frac{[c(b+c)-1]^2}{[c(b-c)+1]^2}\right\},$$

where $b^2 \;=\; \eta^2+c^2-1$ and $c \;=\; \cos(\theta)$.

Some surfaces have two or more scales of roughness, controlled by the slope m (with $m \in \mathbb{R}^+$), and can be modelled by using two or more distribution functions [BS63]. In such cases, D is expressed as a weighted sum of the distribution functions, each with a different value of m parameter. When m is small, the microfacet normals distribute mainly towards the reflection direction. As m value grows, the distribution expands and becomes more uniform. Typically, D is a Gaussian distribution:

$$D(\mathbf{h}) \;=\; \cos(\beta)\,e^{-\left(\frac{\alpha}{m}\right)^2}$$

The geometrical attenuation factor G accounts for the *shadowing* and *masking* of one microfacet by the other side of the microfacet. Its definition is identical to the Torrance-Sparrow model (see section 3.1, page 6). Finally, the specular component is:

$$f_{r,s}(\mathbf{w}_o, \mathbf{w}_i) = \frac{F(\beta)}{\pi} \frac{D(\mathbf{h})\, G(\mathbf{w}_o, \mathbf{w}_i)}{\cos(\mathbf{w}_o)\cos(\mathbf{w}_i)}$$

The main disadvantage of this model, compared to other BRDF representations, is that the parameters are not intuitively set. The user needs to experiment with the values until a good result is found. Another drawback of the model is that the function is not plausible because for some angles this BRDF does not obey the energy conservation law.

The Kajiya BRDF

The Kajiya model [Kaj85] implements an anisotropic method that estimates the analytical form of the reflected intensity light. It is based on Kirchoff's approximation and a stationary base method for the approximation of the radiance equation (Eq. 9), and is considered a model with high computational costs as it is noted in table 1.

The model considers a simplified rough surface that uses the nearest tangent plane. In this work, Kajiya calculates and stores the reflectance in a table each time a surface illumination is evaluated. Later, values from the table are used to perform linear interpolation. Though he uses a novel numerical technique that explores unpolarized light's properties and the Fresnel term, this model shows a lack of many important inter-reflection phenomena. Moreover, conservation of the energy is not guaranteed.

The Poulin-Fournier BRDF

Poulin and Fournier [PF90] introduced a model for anisotropic materials that considered reflection and refraction of the incident light. Anisotropy is represented by a set of parallel cylinders packed tightly together such as those used in [MH84], whose optical properties —and thus the degree of anisotropy— are described by varying the height and distance of these cylinders. The surface is modelled by a distribution of cylinders that are added or subtracted from the base surface. The phenomenon of reflection or refraction happens at the longitudinal cut of the cylinder, more specifically, at the binormal plane BN where $\mathbf{b} = \mathbf{n} \times \mathbf{t}$, so we assume the local system is formed by $\mathbf{n}$, $\mathbf{t}$ and $\mathbf{b}$ vectors (see Figure 3 right in page 7).

To control the degree of anisotropy, this model uses two parameters: distance between cylinders $d \in [0, \infty]$, and height from the base surface $h \in [0, 1]$. Both are unit less and appear in Figure 4. When $d = 0$, this model is the Torrance-Sparrow BRDF. When $d = 2$, the normal of the cylinders differentiate in π and we get the maximum anisotropy. However, if $d > 2$ an imaginary base surface with a constant normal vector appears, and takes a role in the reflection of the light. The base surface is modeled with a classic combination of diffuse reflected intensity $\cos(\mathbf{w}_i)$ and the $\cos(\mathbf{h})^n$ term of the Blinn model to consider the light reflected specularly. The height of the base surface is then controlled with the h parameter. Increasing h causes the decrease of normal variation, thus softening the anisotropy effect.

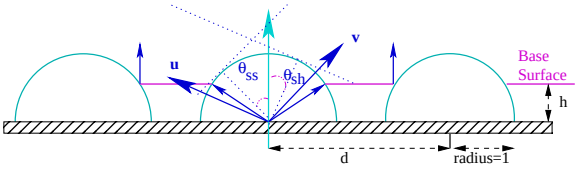

Figure 4: *Anisotropy is controlled with the distance and height parameters.*

The amount of reflected light is calculated by determining the visible and illuminated portion the cylinder on the incident light, as well as reflected by the visible part of the base surface when it intervenes. To make these calculations is necessary to know the length of the projection of the cylinder on the base, visible and illuminated part of the cylinder, as well as the visible and illuminated part of the base surface. The model also considers the shadowing and masking effects of light. You need to know the angles where the cylinder begins to hide himself from the direction of observation θ_{sh}, or by other cylinders. Similarly angles are calculated at which cylinder starts to block light toward the viewer, due to himself θ_{ss}, or by those cylinders at its side.

The calculation for the refraction event is the same with a simple exception: the cylinders are negative or modelled in reverse. In Figure 6 third column two examples of the plot of this function are shown. This model is not energy conserving and its visual results depends upon knowing how to set the parameters correctly, as for the rest of the BRDF models.

The He-Torrance-Sillion-Greenberg BRDF

One of the most complete and complex physical BRDF models is the one of He et al. [HTSG91]. It considers important phenomena associated with the wave-like nature of light such as diffraction and interference. Many parameters contribute to the representation of isotropic materials. Some are geometrical, such as angles, and are illustrated in Figure 3, and others are physical, for example the wavelength λ of the incident beam, the index of refraction η (used in the Fresnel term calculation) and parameters σ and τ to characterize the roughness.

This BRDF starts by distinguishing three components in the reflection event: the uniform diffuse reflection, the perfect specular, and the directional diffuse reflection component. The authors describe an implementation based on spherical harmonics decomposition (see section 4.4) and the Kirchoff's theory for the rough surface analysis. They are used both to approximate the reflectance distribution functions f_r^{ud} and f_r^{dd} and directional intensity distributions for illuminated surfaces. The perfect specular component f_r^{sp} is

represented by the Fresnel equations. By summing the expression of the three components we get the complete BRDF equation:

$$f_r(\mathbf{w}_o,\mathbf{w}_i) = a(\lambda) + \frac{|F(\theta_{\mathbf{w}_o})|^2 \exp(-g(\sigma,\lambda))\, S(\tau)}{\cos(\mathbf{w}_i)} \cdot \eth + \frac{\mathcal{F}(\mathbf{b},\mathbf{p}) S(\tau)}{\cos(\mathbf{w}_o)\cos(\mathbf{w}_i)} \cdot \frac{\tau^2}{16\pi} \cdot \sum_{m=1}^{\infty} \frac{g^m \exp(-g(\sigma,\lambda))}{m!\cdot m} \exp\left(\frac{\mathbf{w}_x^2\tau^2}{4m}\right)$$

where a is the ambient wavelength function, g is the effective surface roughness, σ is a parameter for the amplitude of the roughness, S is a shadow function, τ is a parameter defining the autocorrelation length, $\eth$ is a delta dirac function, $\mathcal{F}$ is a function derived from the Fresnel function, $\mathbf{b}$ is the bisected unit vector, $\mathbf{p}$ is the incident polarization state vector and $\mathbf{w}$ is the wave vector change.

Detailed mathematical construction is included in [HTSG91], experimental analysis can be found in [NDM05]. Although at present is not an issue to consider, at the time of this model the computational cost was high and required optimizations based on precalculus and search tables [HHP*92]. In attempts to make it more usable, simplifications have been made in the formulation [WAT92] and spherical wavelets has been used to represent this BRDF. This idea is detailed in section 4.5.1. The He et al. BRDF is theoretical, not reciprocal and since it has no associated direct sampling method (as table 1 shows) is not usually integrated into Monte-Carlo based systems.

The Oren-Nayar BRDF

The Oren & Nayar model [ON94, ON95] is an improvement on the classical Lambertian interpretation for a diffuse material. This model is able to explain the view dependence appearance of the matte surfaces with geometric optics, and for this reason the BRDF is classified as physical or theoretical.

In this case the *microfacet* or groove distribution is purely diffuse. In addition to *masking* and *shadowing* light blocking events, the reflections between *microfacets* are also considered, but they have a limited number of bounces within each pair of *microfacets*. The orientation of the grooves is distributed according to a Gaussian function with a standard deviation for the angles α_m (in radians), which is a measure of the roughness of the surface. It ranges from 0 to 1. The dirty materials tend to more reflect the light to backward of the light(retroreflection). This characteristic is controlled with parameter α_m. The larger α_m, the more retro-reflective is the material.

Given an incident direction, the total reflected radiance is the integral of grooves' reflectance values —the projected reflected radiance— and the radiance due to the bounces between them. Oren & Nayar found hard to solve the resulting equations analytically, so they presented a functional approximation:

$$f_r(\mathbf{w}_o,\mathbf{w}_i) = \frac{\rho}{\pi}\left(A + B\max(0,\cos(\phi_{\mathbf{w}_i} - \phi_{\mathbf{w}_o}))\sin(a)\tan(b)\right)$$

where $a = \max(\theta_{\mathbf{w}_o},\theta_{\mathbf{w}_i})$, $b = \min(\theta_{\mathbf{w}_o},\theta_{\mathbf{w}_i})$, and:

$$A = 1 - 0.5\frac{\alpha_m^2}{\alpha_m^2+0.33} \qquad B = 0.45\frac{\alpha_m^2}{\alpha_m^2+0.09}$$

In the case of $\alpha_m = 0$, roughness is null and the previous expression is equivalent to the *Lambert Law* (also $A = 1$, $B = 0$). Application of trigonometry transformations can substantially improve the implementation of this BRDF.

The Coupled BRDF

Shirley et al. [SHSL97] introduced a model for the representation of matte surfaces. It is called a *coupled model* because it properly combines the diffuse and specular reflections. It is plausible, physically based and suited for Monte-Carlo rendering algorithms. The model for specular reflection assumes a polished planar surface of dielectrics in touch with the air. The matte component is considered to be almost constant and isotropic, so both are combined as follows:

$$f_r(\mathbf{w}_o,\mathbf{w}_i) = F(\theta_{\mathbf{w}_o}) + k R_m f(\theta_{\mathbf{w}_o}) f(\theta_{\mathbf{w}_i})$$

where k is a constant for normalization and R_m is the reflectance of the matte component given as a parameter of the model. Finally $f(\theta)$ is approximated with the Schlick approximation of the Fresnel term [Sch94a] as follows:

$$f(\theta) \propto (1 - (1-\cos(\theta))^5)$$

Restrictions are imposed to guarantee energy conservation as if the Fresnel term at grazing angles tends to one, the diffuse component should tend to zero:

$$R_0 + 2\pi k \int_0^{\frac{\pi}{2}} f(\theta_{\mathbf{w}_i}) d\sigma(\mathbf{w}_i) = 1$$

allowing the authors to solve k:

$$k = \frac{21}{20\pi(1-R_0)}$$

where R_0 is another parameter that varies between 0.03 and 0.06. We arrive at:

$$f_r(\mathbf{w}_o,\mathbf{w}_i) = [R_0 + (1-\cos(\mathbf{w}_o))^5 (1-R_0)]\, f_{r,s}(\mathbf{w}_o,\mathbf{w}_i) + k R_m [1-(1-\cos(\mathbf{w}_o))^5][1-(1-\cos(\mathbf{w}_i))^5]$$

The Ashikhmin-Shirley BRDF

Ashikhmin & Shirley [AS00] developed an anisotropic microfacet model that uses simple and intuitive parameters. Basically you can generate any BRDF from a distribution of microfacets which is generally expressive. They also provided a method of sampling based on the BRDF function. Two parameters define the anisotropy by controlling the halfway vector distribution of the microfacets. These parameters are related to the axes of an ellipse: e_x and e_y that orientate $\mathbf{h}$ along the X and Y axes respectively. An exponent value e is calculated with respect to the ellipse radius and the ϕ angle of orientation. The distribution function is as follows:

$$D(\mathbf{h}) = \sqrt{(e_x+1)(e_y+1)}\,(\mathbf{h}\cdot\mathbf{n})^{e_x\cos^2(\phi_{\mathbf{h}}) + e_y\sin^2(\phi_{\mathbf{h}})}$$

Applying trigonometry rules, a simplification of the exponent of $D(\mathbf{h})$ is achieved. Note that the following expression

are undetermined when $z_{\mathbf{h}} = 1$.

$$\cos^2(\phi_{\mathbf{h}}) = \frac{x_{\mathbf{h}}^2}{1-z_{\mathbf{h}}^2} \qquad \sin^2(\phi_{\mathbf{h}}) = \frac{y_{\mathbf{h}}^2}{1-z_{\mathbf{h}}^2}$$

In [APS00] the authors complement the previous BRDF model with one for diffuse surfaces covered with a polished or painted layer. For example a wooden table with lacquer paint. At normal incidence it is diffuse but at the horizontal view it is almost specular. The Fresnel equations describe this very phenomenon, and it is modelled with a superposition of two layers: one specular and one diffuse.

The BRDF is expressed as a weighted sum of the specular term and the diffuse one: $f_r = f_{r,s} + f_{r,d}$. For the specular reflection, the distribution over $\mathbf{h}$ is used as well as the Schlick's approximation of the Fresnel term [Sch94b]:

$$f_{r,s}(\mathbf{w}_o, \mathbf{w}_i) = \frac{D(\mathbf{h})\, F(\mathbf{w}_i)}{8\,\pi\,(\mathbf{h}\cdot\mathbf{w}_o)\,\max(\cos(\mathbf{w}_o), \cos(\mathbf{w}_i))}$$

The diffuse term guarantees the reciprocity and energy conservation properties, so the BRDF is plausible.

$$f_{r,d}(\mathbf{w}_o, \mathbf{w}_i) = \frac{28 k_d}{23\pi}\,(1-\rho_s)\,\Lambda(\mathbf{w}_o)\,\Lambda(\mathbf{w}_i)$$

where

$$\Lambda(\mathbf{u}) = \left(1 - \left(1 - \frac{\cos(\mathbf{u})}{2}\right)^5\right)$$

Two examples of the function plot are shown in Figure 6 first column. Though this BRDF is not symmetric is one of the most complete reflectance function as it also includes a sampling method for the generation of random reflected directions.

Granier-Heidrich BRDF

The Granier & Heidrich BRDF [GH03] is a reflectance model specifically conceived for an easy to evaluate representation of old metals, or dirty surfaces covered with an oily transparent exterior surface. This two layers model uses the wavelength of the incident light to simulate two phenomena:

1. A change of phase between the beam of light that is reflected and the beam of the incident light that is transmitted to the other layer occurs.
2. The index of refraction is wavelength dependent, $\eta(\lambda)$ and produce the dispersion of light in different colors (much like a prism). This is obtained with a model of non-parallel layers, with a different alignment of the normal of the outer surface and the normal of the inner surface.

Though the model is λ dependent, an initial approximation is carried out using the RGB color model with values R = 645 nm, G = 525 nm, and B = 445 nm. Another simplification is associated with the outer layer using η_1 corresponding to the vacuum, with $\eta_1 \leq \eta_2$. This assumption implies that transmission always happens. The final result is a BRDF that combines the reflection term R and the transmission term T. R is a cosine weighted by the reflectivity —the Fresnel term using the Schlick approximation— due to direct illumination. For the transmission term, the reader is referred to the original paper [GH03], where a hardware acceleration technique that uses textures, is also suggested in order to obtain low cost results.

3.2. Empirical Reflectance Models

The Minnaert BRDF

One of the first reflectance models was given by Minnaert [Min41] to model the lunar surface reflectance. This model can be applied not only to the moon, but to shade an object where we would see a darkening of color near the edges. The model is controlled using two parameters: ρ_d and an exponent responsible for darkening k. This shape parameter usually varies between 0 and 2. When $k = 1$, this function is equivalent to the Lambertian function. The analytical expression for this BRDF is:

$$f_r(\mathbf{w}_o, \mathbf{w}_i) = \frac{\rho_d}{\pi}\,(cos(\mathbf{w}_o)\,cos(\mathbf{w}_i))^{k-1}$$

The Phong BRDF

Phong [Pho75] is still a very popular BRDF model and it was the first description for non-Lambertian surfaces. Is a well-known class of BRDF models based on cosine-lobes where the term lobe here refers to the shape of a classic Phong-like BRDF as is shown in Figure 6 second column. Basically, it is an empirical model which obeys neither energy conservation nor reciprocity, but its simplicity has made it one of the most used in Computer Graphics. It depends on an α angle, which is calculated after reflecting the incident direction. Essentially, this model is a simplification of the Torrance-Sparrow one, where the G and F factors are dropped and the distribution D is reduced to:

$$D(\mathbf{w}_o, \mathbf{w}_i) = (\mathbf{w}_o \cdot \mathbf{r}_{\mathbf{w}_i})^n$$

where the parameter $n \in [0, \infty[$ characterizes the shape of the specular highlight (from 0 or dull to more glossy surface). Furthermore, this model could be faster with an optimization of the exponential operator, like the one given by Schlick [Sch94a]:

$$\cos^n(\alpha) \approx \frac{\cos(\alpha)}{n - n\cos(\alpha) + \cos(\alpha)}$$

The second and third parameters are the specular k_s and diffuse k_d constants, both taking values in $[0,1]$. They allow a linear combination of the specular lobe with the Lambertian-diffuse BRDF. Precisely the lack of physical significance and the fact of combining the two components linearly, can create situations in which energy is not retained.

$$f_r(\mathbf{w}_o, \mathbf{w}_i) = k_s\,(\mathbf{w}_o \cdot \mathbf{r}_{\mathbf{w}_i})^n$$

The Blinn BRDF

The Blinn BRDF, also known as the Blinn-Phong reflection model, is the standard lighting model used in both the DirectX and OpenGL rendering pipelines. Blinn [Bli77] noted that normally the direction that gave the higher reflection correspond to the halfway vector **h** aligned with the normal. This vector is then used in conjunction with the normal to get the specular highlight.

$$D(\mathbf{h}) \;=\; (\mathbf{n}\cdot\mathbf{h})^n \;=\; \cos(\delta)^n$$

In this way, Phong BRDF is modified replacing $(\mathbf{u}\cdot\mathbf{r})$ by $(\mathbf{n}\cdot\mathbf{h})$, allowing less calculations, because it is not necessary to find the reflection vector. Two examples of the evaluation of this function is shown in Figure 6 second column.

$$f_r(\mathbf{w}_o,\mathbf{w}_i) \;=\; k_s\,(\mathbf{n}\cdot\mathbf{h})^n \; with\; k_d + k_s = 1$$

The Lewis BRDF

Reviewing the previous models, Lewis [Lew94] made a study of their properties. Models like Phong or Cook-Torrance did neither exhibit energy conservation nor reciprocity, and so Lewis elaborated a plausible version of them. With reference to microfacets based surface modelling, the cause of plausibility is the normal distribution D, so it should be normalized in order that the BRDF can be used safely in any lighting algorithm. The total value of the projected *microfacet's* areas should be same as the differential area of the considered surface. If we assume energy conservation, the following should occur:

$$\int_\Omega D(\mathbf{h})\,\cos(\mathbf{h})\,d\sigma(\mathbf{h}) \;=\; 1$$

In the case of the Phong distribution $D(\mathbf{u},\mathbf{v}) = (\mathbf{u}\cdot\mathbf{r}_\mathbf{v})^n$, the normalization factor is $c \;=\; \frac{n+2}{2\pi}$. If we apply this normalization to the Blinn BRDF model, then energy conservation is guaranteed. We name Lewis BRDF to the modified version:

$$f_r(\mathbf{w}_o,\mathbf{w}_i) \;=\; k_s\,\frac{n+2}{2\pi}\,(\mathbf{n}\cdot\mathbf{h})^n$$

We note here that a normalization to the Phong BRDF was given also by Lafortune et al. [LFTG97].

The Neumann-Neumann BRDF

The Neumann-Neumann BRDF model [NN96] explores a plausible function easy to integrate in an Monte-Carlo based rendering algorithm. For the description of metal, plastics, ceramic, or retroreflective material, and even the anisotropic reflectance, the authors built these BRDFs over a base model. They presented two key ideas. The first, was that the base BRDF uses the unit disc domain $\mathcal{D}^2$ and thus the σ_p measure, so a cosine term is implicit. In the second one, the projection P of the reflection vector is the origin of a disc C whose radius is controlled by a parameter r ($r \neq 0$). Figure 5 shows the geometry previously described. The BRDF function is a constant value defined as:

$$f_r(\mathbf{w}_o,\mathbf{w}_i) \;=\; \begin{cases} \frac{1}{\pi r^2} & if\; P(\mathbf{w}_i) \in C(P(\mathbf{r}_{\mathbf{w}_o}),r), \\ 0 & in\; other\; case. \end{cases}$$

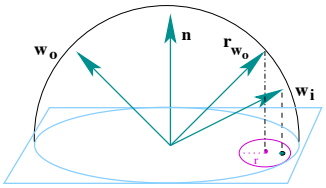

Figure 5: *The Neumann-Neumann BRDF is based on a disc of variable radius defined over $\mathcal{D}^2$ domain.*

The surface may vary from perfect specular $r = 0+\varepsilon$, to perfect diffuse $r = 2$ and the model allows to simple calculation of the *directional-hemispherical reflectance*:

$$\rho(\mathbf{w}_o) \;=\; r\cdot Area(C(P(\mathbf{r}_{\mathbf{w}_o}),r)).$$

Using the base model it is easy to build other BRDFs. For example a retroreflective one would simply change the **h** of the distance function by $\mathbf{g} \;=\; \mathbf{w}_o - \mathbf{w}_i$. As a consequence, light will reflect predominantly in the incident direction. Another example is a BRDF for anisotropic surfaces which change the circle C by an ellipse E whose axes are A and B, and the distance function by the normal elliptic curve.

$$f_{r,aniso}(\mathbf{w}_o,\mathbf{w}_i) \;=\; \begin{cases} \frac{1}{ab\pi} & if\; P(\mathbf{w}_i) \in E(P(\mathbf{r}_{\mathbf{w}_o}),a,b),\;\; b \leqslant B/A \\ \frac{1}{Area(E)} & if\; P(\mathbf{w}_i) \in E(P(\mathbf{r}_{\mathbf{w}_o}),a,b),\;\; B/A < b \leqslant 2 \\ 0 & in\; other\; case. \end{cases}$$

The Strauss BRDF

The Strauss BRDF [Str90] is an empirical model that characterized metals, and other glossy surfaces that exhibit *off-specular peaks*. Strauss noted on previous BRDF models how difficult it was to select the correct values for those BRDFs when wishing to mimic the appearance of a material. His model is based on few and very intuitive parameters that represent different types of material properties that any user should be able to set without problems.

- Chromatic color C or surface color (in $[0,1]$).
- Specular color C_s is the calculated (not a parameter) shiny color.
- Smoothness: when $s = 0$ we have the perfect diffuse surface, and when $s = 1$, the surface behaves like a mirror. This value changes the ratio from diffuse to specular and also the shape of the specular highlight.
- Metalness: when $m = 1$ the surface is full metallic, and when $m = 0$ we have the absence of this property. It changes the diffuse aspect of the resulting image and also it is involved in the computation of the specular color.
- Transparency: when $t = 0$ you get a totally opaque surface, when $t = 1$ all light not reflected will be transmitted through the media. The transmittance value used is the value of t at normal incidence direction.
- Index of refraction η: employed to compute the direction of the transmitted beam of light.

The Strauss reflectance model uses a linear combination of diffuse and specular components controlled by two coefficients k_d and k_s.

$$\begin{aligned} f_r(\mathbf{w}_o,\mathbf{w}_i) &= k_d\, f_{r,d}(\mathbf{u},\mathbf{v}) + k_s\, f_{r,s}(\mathbf{w}_o,\mathbf{w}_i) \\ &= k_d\cos(\mathbf{w}_i)\, d\, r_d\, C + k_s\, r_s\, C_s \end{aligned}$$

In order to obtain the values needed, the model performs some simple operations:

$$\begin{aligned} r_d &= (1-s^3)(1-t) & d &= (1-ms) \\ r_n &= (1-t) - r_d & e &= \tfrac{3}{1-s} \\ r_j &= min[1, r_n + (r_n + k_j)\, j] & k_j &= 0.1 \\ r_s &= [-(\mathbf{h}\cdot\mathbf{w}_i)]^e\, r_j & j &= F(\alpha)\, G(\alpha)\, G(\delta) \end{aligned}$$

The meaning of r_j is similar to the Fresnel term together with the geometric term. It uses two constant values $k_f = 1.12$ and $k_g = 1.01$, as well as a cosine term $x \in [0,1]$. The model precomputes F and G, keeping its simplicity. It also assumes that for metals, the color of the reflection should not be the same as the color of the surface, and thus:

$$C_s = \begin{cases} C_1 & if\ non-metal \\ C_1 + m(1 - F(\alpha))(C - C_1) & if\ metal \end{cases}$$

where C_1 is the equivalent to white specular color that is acquired at $\pi/2$ incidence angle.

3.3. Experimental Reflectance Models

The Ward BRDF

Previous BRDF models that account for anisotropy were computationally expensive so Ward [War92] developed a device to acquire the reflectance of a surface sample, as well as a mathematical description of the reflectance of anisotropic materials. The Ward BRDF uses a Gaussian lobe controlled by the standard deviation. For the isotropic version of the model this parameter is α_m. The model uses the halfway vector $\mathbf{h}$ and two constants for the combination of the diffuse and specular components of the reflection. This BRDF can be validated using experimental measurements. The mathematical expression is:

$$f_{r,iso}(\mathbf{w}_o,\mathbf{w}_i) = \frac{k_s}{\sqrt{\cos(\mathbf{w}_o)\cos(\mathbf{w}_i)}} \frac{exp\left[-\tan^2\left(\frac{(\mathbf{h}\cdot\mathbf{n})}{\alpha_m^2}\right)\right]}{4\pi\alpha_m^2}$$

Note that the exponent is zero in the case of the ideal reflection. The normalization factor $\frac{1}{4\pi\alpha_m^2}$, guarantees the correct integration of this function on the hemisphere of directions. Because of the Gaussian, the model produces quite high values —which should be avoided in a rendering system— specially when α_m is around 0.2 at grazing viewing angles [MWM*98]. The behavior of the Ward model at grazing angles has been discussed in [NNSK99, GMD10]. The use of the normalization term prevents for these numerical instabilities, but the given here is not the only. In [Dür06], a study on the energy conservation of the Ward BRDF results in other possibilities for normalization.

The anisotropic version of the mathematical formulation [Wal05] uses an elliptic Gaussian whose axes are aligned in a way that is controlled by parameters α_x and α_y.

$$f_{r,ani}(\mathbf{w}_o,\mathbf{w}_i) = \frac{k_s}{4\pi\alpha_x\alpha_y\sqrt{\cos(\mathbf{w}_o)\cos(\mathbf{w}_i)}}\, e^{\left[-\frac{\left[\frac{(\mathbf{h}\cdot\mathbf{x})}{\alpha_x}\right]^2+\left[\frac{(\mathbf{h}\cdot\mathbf{y})}{\alpha_y}\right]^2}{(\mathbf{h}\cdot\mathbf{n})^2}\right]}$$

where

$$(\mathbf{h}\cdot\mathbf{x}) = \frac{\sin(\theta_{\mathbf{w}_o})\cos(\phi_{\mathbf{w}_o}) + \sin(\theta_{\mathbf{w}_i})\cos(\theta_{\mathbf{w}_i})}{|\,\mathbf{h}\,|}$$

$$(\mathbf{h}\cdot\mathbf{y}) = \frac{\sin(\theta_{\mathbf{w}_o})\sin(\phi_{\mathbf{w}_o}) + \sin(\theta_{\mathbf{w}_i})\sin(\phi_{\mathbf{w}_i})}{|\,\mathbf{h}\,|}$$

$$(\mathbf{h}\cdot\mathbf{n}) = \frac{\cos(\theta_{\mathbf{w}_o}) + \cos(\theta_{\mathbf{w}_i})}{|\,\mathbf{h}\,|}$$

$$\begin{aligned} |\,\mathbf{h}\,| = [&2 + 2\sin(\theta_{\mathbf{w}_o})\sin(\theta_{\mathbf{w}_i})\,(\cos(\phi_{\mathbf{w}_o})\cos(\phi_{\mathbf{w}_i}) + \\ &\sin(\phi_{\mathbf{w}_o})\sin(\phi_{\mathbf{w}_i})) + 2\cos(\theta_{\mathbf{w}_o})\cos(\theta_{\mathbf{w}_i})]^{\frac{1}{2}} \end{aligned}$$

This BRDF is not plausible but is one of the most versatile reflectance functions as is cheap to evaluate, has a direct sampling method and fits well to measured reflectance data. Examples of its 3D plot are found in Figure 6 fifth column; the fourth column shows examples of our next reflectance model.

Variants have been developed more efficient computationally, better suited for fitting measuring reflectance data and efficient for Monte-Carlo importance sampling (see section 5). It is the case of the Ward-Dür BRDF model for specular anisotropic reflection [GMD10].

The Schlick BRDF

The objective of the Schlick-BRDF [Sch93, Sch94b] is a plausible model which is based on the microfacets model, the Fresnel equations and the set of parameters also allow the distinction between isotropy and anisotropy. Schlick proposes an alternative way to [SHSL97] of representing heterogeneous surfaces: using a two layer model. The outer layer is used for specular reflection and the inner one is for diffuse subsurface scattering. Homogeneous surfaces are represented by the *single* layer model with values (C_λ, r, p). A heterogeneous surface should use the *double* layer model with values (C_λ, r, p) and (C'_λ, r', p'), where:

- C_λ is the reflectance which depends on λ, and gives values between 0 and 1.
- $r \in [0,1]$ describes the roughness. When $r = 0$ it represents a mirror; if $r = 1$ we have the perfect diffuse surface.
- $p \in [0,1]$ describes the isotropy. When $p = 0$ is full anisotropy and if $p = 1$ is full isotropy.

The meaning of these parameters is the same in both the single or double layer model. This implies that the computation of $S(u)$ in C_λ and $S'(u)$ is the same for C'_λ, only the

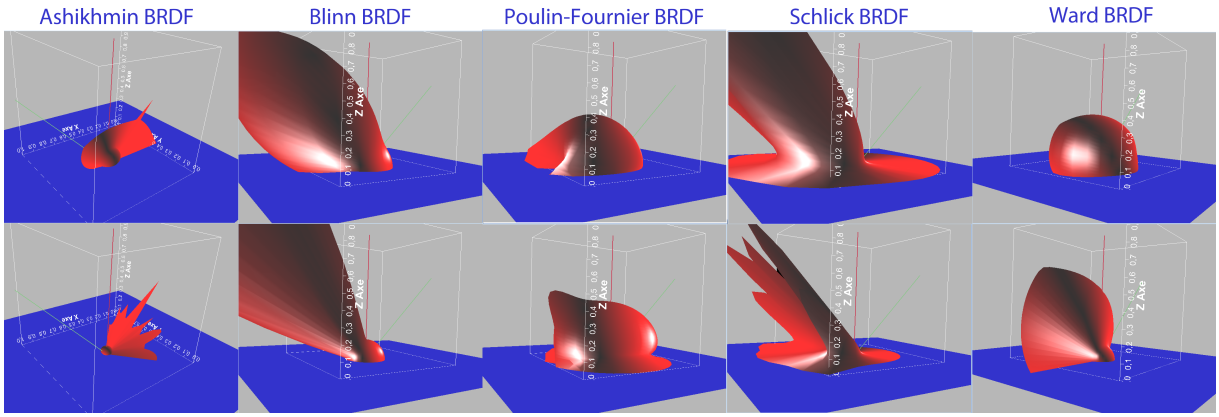

Figure 6: *Some examples of 3D plot of BRDF models. From left to right: Ashikminn-Shirley with parameters nu* $= 1$*, nv* $= 75$*, ks* $= 0.5$*, kd* $= 1$ *(up) and nu* $= 75$*, nv* $= 1$*, ks* $= 0.7$*, kd* $= 0.7$ *(down); Blinn ks* $= 0.3$*, kd* $= 0.7$*, n* $= 15$ *(up) and ks* $= 0.5$*, kd* $= 0.5$*, n* $= 100$ *(down); Poulin-Fournier d* $= 2$*, h* $= 0.01$*, n* $= 10$*, ks* $= 0.8$*, kd* $= 0.2$ *(up) and d* $= 4$*, h* $= 0.2$*, n* $= 200$*, ks* $= 0.8$*, kd* $= 0.5$ *(down); Schlick single layer* $[0.3, 0.1, 0.2]$ *(up) and double layer* $[0.05, 0.17, 0.11][0.12, 0.4, 0.1]$ *(down).*

parameter value differs. The BRDF model is expressed as:

$$f_r(\mathbf{w}_o, \mathbf{w}_i) = R((\mathbf{n}\cdot\mathbf{h}), (\mathbf{w}_o\cdot\mathbf{h}), (\mathbf{w}_i\cdot\mathbf{n}), (\mathbf{w}_o\cdot\mathbf{n}), \phi_{\mathbf{h}})$$

where the arguments of the reflectance function R are substituted by (t,u,v,v',w) for its calculus. We have $R(t,u,v,v',w) = S(u,C_\lambda)\,D(t,v,v',w)$ in the case of using the single layer model and for the double layer it is extended as:

$$R(t,u,v,v',w) = \begin{array}{l} S(u,C_\lambda)\,D(t,v,v',w) + \\ [1-S'(u,C'_\lambda)]\,S'(u,C'_\lambda)\,D'(t,v,v',w) \end{array}$$

Here the specular term $S(u,C_\lambda)$ is an approximation of the Fresnel term and $D(t,v,v',w)$ is the directional term that accounts for emission and re-emission of light at subsurface levels. The directional term contemplates the geometry of the microfacets $G(v,r)$, and models the anisotropy with a dependence on the zenith angle, $Z(t,r)$, and the azimuthal angle $A(w,p)$. The directional term is expressed as:

$$D(t,v,v',w) = \frac{G(v)\,G(v')}{4\pi\,v\,v'}\,Z(t)\,A(w) + \frac{(1-G(v)\,G(v'))}{4\pi\,v\,v'}$$

In addition to providing the previous function, Schlick introduced in [Sch94a] a computationally effective approximation to Fresnel's equations, which was widely used in other models and is present in nowadays applications.

The Lafortune BRDF

One of the most multifunctional BRDF models is the one introduced by Lafortune et al. [LFTG97]. It was used to fit measurements from real surfaces and can be considered as a generalization of the Phong BRDF [Pho75] that is reciprocal and obeys the energy conservation law. With the reflection operator around the normal direction $\mathbf{r_u} = 2(\mathbf{u}\cdot\mathbf{n})\,\mathbf{n} - \mathbf{u}$, expressed in a canonical reference system, $\mathbf{r_u}$ is equal to $(-x_\mathbf{u}, -y_\mathbf{u}, z_\mathbf{u})$, which is interpreted as a scale factor (-1,-1,1) applied to the original vector. When we apply the generalization, a matrix M is used for the reflection operator and thus $f_r \propto (\mathbf{w}_i\cdot M\mathbf{w}_o)^n$. The modified Phong expression is:

$$f_r(\mathbf{w}_o, \mathbf{w}_i) = (\mathbf{w}_o\cdot\mathbf{r}_{\mathbf{w}_i})^n = (\mathbf{w}_i\cdot\mathbf{r}_{\mathbf{w}_o})^n$$

If we express the diagonal of a matrix M as a vector $\mathbf{o}$ — note that this is a parameter of the model— a retroreflection effect is obtained with $\mathbf{o}$ set to (1,1,1). By using more than one lobe, this BRDF is able to represent the data from acquired materials. Let N be the number of lobes, which is used in the final expression:

$$f_r(\mathbf{w}_o, \mathbf{w}_i) = \frac{\rho_d}{\pi} + \sum_{l=1}^{N} (\mathbf{w}_i\cdot(x_\mathbf{u}x_{\mathbf{o}_i}, y_\mathbf{u}y_{\mathbf{o}_i}, z_\mathbf{u}z_{\mathbf{o}_i}))^{n_l}$$

4. Function Approximation for Acquired BRDF models

Suitable analytic models are not always available for a desired type of surface. Sometimes their formulation does not make them useful in a rendering system. To overcome these limitations, a number of researchers have proposed and used techniques for obtaining BRDF models from measured reflectance data. This strategy allows integration of realism in global illumination rendering systems by using data from real materials. However raw tabulated reflectance data cannot be directly used in rendering systems because it requires a considerable amount of memory and processing time, due to the high dimensionality of the problem domain.

A common solution to this problem is to choose a suitable function space, and adapt algorithms to approximate measured BRDF functions in that space. In this line, some strategies which have been specifically designed include:

- Basis functions, such as a single Gaussian lobe [War92], or summation of cosine lobes [LFTG97].
- Spherical harmonics [WAT92, KSS02].

- Weighted sum of separable functions [Fou95, KM99, LRR04].
- Zernike polynomials [KvDS96].
- Spherical wavelets [LF97, CBP02, CPB03, CPB06].
- Product of functions (factorization) [MAA01, LK02].

Acquisition of BRDFs can be carried out using a gonioreflectometer [War92, GA97], a device capable of measuring a BRDF by moving a light and a sensor through different positions in the space of incoming light and outgoing reflection (captured by the device), taking measurements every few degrees. After, a denoising preprocessing, a tabulated BRDF is obtained. Other researchers have worked towards BRDF acquisition methods based on simpler devices, allowing to measure material reflectance by using a single digital camera in combination with curved mirrors [Dan01]. Also, we could use computer simulation or emulation of light propagation in a given type of material, by developing adequate models of those materials [CMS87, WAT92, APS00].

After raw data has been obtained (usually a set of reflectance values corresponding to a set of pairs of incoming and outgoing directions in the hemisphere), it is necessary to filter it to eliminate noise, and then find the closest approximation in the given function space. This can be done by projection (for function spaces spawned by orthonormal basis sets) or using non-linear function fitting techniques for other schemes. Usually, the need to save memory implies that some compression scheme should be used, finding an adequate trade-off between approximation quality and memory consumption.

Fitting is carried out by numerical optimization techniques which minimize the error between modelled (f') and measured data (f). As stated, measured data is a set of n reflectance values $\{f_1, f_2, \ldots, f_n\}$ obtained for some set of n sample directions pairs, while f' is a function which can be evaluated for those sample directions yielding another set of n values $\{f'_1, f'_2, \ldots, f'_n\}$. The goal of function approximation is to find a function f' which minimizes the distance between f' and f. Two error metrics are commonly used:

$$\text{RMS error} \quad \sigma = \sqrt{\frac{1}{n}\sum_i \left(f'_i - f_i\right)^2}$$

$$\text{relative RMS error} \quad \sigma_r = \sqrt{\frac{1}{n}\sum_i \left(\frac{f'_i - f_i}{f_i}\right)^2}$$

although relative RMS seems more appropriate, we must take into account that for this metric it is necessary to exclude those samples from the summation for which $f_i = 0$, even when $f'_i \neq 0$. The error metric [NDM05] also could be used as the L^2 metric over the incident and outgoing hemispheres of directions. This metric has an advantage when applied to measurements as it is able to remove the part of the domain where data is not reliable. This situation could occur with extreme grazing angles (angles larger than 80 degrees) [NDM05].

Function approximation can also be used to approach known analytical BRDF models, because this allows to handle a very wide class of BRDFs by using an uniform approach in rendering systems. Fitting exact known analytical models is also used to verify validity and performance of function approximation strategies.

Actually measured reflectance data is publicly available from various sources, such as the initial Ward's data set [War92], the CUReT (Columbia-Utrech) [DGNK99], the Cornell graphics laboratory (http://www.graphics.cornell.edu) or the MIT's MERL database [MPBM03]. These data sets differ considerably in many aspects, such as the file format or the number of samples acquired. In this section we review the literature to show the strategies used for BRDF approximation in function spaces.

4.1. Basis Functions

Specular BRDFs can be approximated by a single Gaussian lobe, as described in [War92] or by using a summation of generalized Phong lobes [LFTG97] (both in section 3.3) or adjusting to other analytical BRDF models such as Cook-Torrance, Blinn-Phong or He et al. This type of representation consists of fitting some primitive function to a physically-based model or to actual reflectance measurements. The representation must be positive, reciprocal and energy conserving.

When the basis functions are non-linear, a non-linear optimization technique is required to determine the parameters of the BRDF. In this case we want to minimize the mean-square error of the reflectance function, and usually the Levenberg-Marquardt technique [GMW81] is applied. This is in essence a good option as it needs fewer terms of coefficients than other methods, given that a single function can capture a complete BRDF over its incident and outgoing direction domain, thus it is uniform and compact. In case of the generalized Phong lobes [LFTG97], two or three coefficients and an exponent are needed.

This representation possesses many qualitative and quantitative properties. It is able to represent the directional diffuse reflection: (1) the fading out of the diffuse component for grazing angles, (2) the specular mirror term at grazing angles, (3) retro-reflection —scattering in the backward direction—, and (4) the off-specular reflection —maximum directional-diffuse lobe at the grazing direction—. Usually, this type of representation omit the Fresnel factor and the fit of analytic reflectance data can result in significant error.

As an alternative, we could use a linear model for approximating BRDFs. In [OKBG08], isotropic and anisotropic reflectances can be achieved with a simple and efficient model which avoids complicated parameters or non-linear optimization processes by employing polynomial functions.

4.2. Separable Decomposition or Factorization

Factorization techniques represent the BRDF using lower dimensional functions, generally as a sum of them, though

in the next section we introduce some techniques using the product of the terms. Each term is the product of two functions, one of the incident direction and other of the reflected direction.

Representations based on dimensionality reduction have to construct a full sample matrix and perform basis decomposition. This process could become significantly costly if dense scattered data is used, but is suitable for representing measured data with generic analytical models achieving high compression rates. By approximating a BRDF table with a set of factors we can significantly reduce storage requirements and create a data format more suited to graphics hardware. The factorization procedure decomposes the BRDF function into a sum of terms, generally expressed as:

$$f_r(\mathbf{w}_o, \mathbf{w}_i) \approx \sum_{k=1}^{N} g_k(\mathbf{w}_o) h_k(\mathbf{w}_i) \tag{14}$$

Computation of factors can be done analytically or numerically and in the case of real-time rendering they are stored in texture maps. There are various ways to achieve an analytical decomposition in the sum of products: from Taylor series expansion to spherical harmonics [WAT92], Zernike polynomials [KvDS96], K-means clustering [LM01] or as a simple and universal numerical approach as singular value decomposition (SVD).

Given a large enough number of factors, any BRDF can be approximated to arbitrary accuracy. However, we need a shortened series of factors which should be optimal for computational use. For this reason researchers have devised many factorization schemes. The numerical algorithm used to compute each factor is another source of variation. In the following subsections we review some of them.

4.2.1. Usage of Singular Value Decompostion

The use of singular value decomposition (SVD) was presented in [Fou95, Rus98]. Given a matrix M (of size $p \times q$, $p > q$) this process decomposes it into the product of three matrices $M = UWV^T$. With the use of SVD each element of M is seen as a weighted sum of the rows of U and the columns of V^T. In the case of the BRDF we take a function of four variables and separate them into the sum of the products of the two two-variable functions: p pairs of $(\theta_{\mathbf{w}_o}, \phi_{\mathbf{w}_o})$ for the outgoing direction and q pairs of $(\theta_{\mathbf{w}_i}, \phi_{\mathbf{w}_i})$ for the incoming direction if $M_{i,j} = f_r(\mathbf{w}_o, \mathbf{w}_i)$. This decomposition obeys reciprocity in [Rus98]. The Phong BRDF and Ward's experimental data was approximated by the authors to be used for radiosity calculations. Nonetheless with SVD, the existence of positive and negative factors can lead to inadequate results and complicate the parametrization. The presence of negative factors also prevents its use for BRDF sampling purposes, and clampping these values will not solve the original problematic.

4.2.2. Normalized decomposition on graphics hardware

Kauzt and McCool [KM99] proposed an approximation of the BRDF based on textures, expanding the technique of [Fou95]. This is a compressed representation that uses naive two-dimensional hardware texture capabilities to achieve interactive rates of rendering. In this case the two-dimensional functions are held in texture maps. They evaluate two algorithms for finding appropriate functions for g and h (terms of Eq. (14)): SVD and normalized decomposition (ND). The fact that SVD introduces negative terms is numerically problematic and is not compatible with the strictly positive nature of the reflectance. The normalized decomposition is considerably faster than SVD, takes less memory and contains only positive factors.

To improve the BRDF separability, it is recommended a change of parametrization to align the main features of the BRDF in the matrix representation. The Rusinkiewicz's reparametrization or the elevation/azimuth works well for analytical and acquired reflectance data but is incompatible with the texture coordinate computations of the hemisphere-maps. In real-time rendering, the best solution for hardware accelerations is to use the Gram-Schmidt half-vector parametrization. (See section 2.1 for a description of those parametrizations). With this representation it is quite easy to evaluate the BRDF at a specific pair of directions, as it requires few texture lookups, multiplications and additions.

4.2.3. Product of lower dimensional factors

The BRDF factorization given by Lawrence et al. [LRR04] divides the BRDF function into the product of lower dimensional factors, stored in a tabular and compact form. Furthermore, they introduced a novel BRDF sampling procedure. The BRDF expression use two distinct factorizations:

$$f_r(\mathbf{w}_o, \mathbf{w}_i) \cos(\mathbf{w}_i) \approx \sum_{j}^{J} F_j(\mathbf{w}_o) \sum_{k}^{K} U_{jk}(\theta_{\mathbf{w}}) V_{jk}(\phi_{\mathbf{w}}) \tag{15}$$

where $\mathbf{w}$ is a sampled random vector. The choice of $\mathbf{w}$ (the parametrization) will depend on the features or complexity of the BRDF. In the case of diffuse BRDFs, it is better to use $\mathbf{w}$ as the local representation of $\mathbf{w}_i$. For more specular BRDFs, is preferable to use $\mathbf{w}$ as $\mathbf{h}$ in order to align important properties such as the highlights.

The initial data matrix Y contains $N_{\mathbf{w}} \times N_{\mathbf{w}_o}$ samples of the BRDF along the outgoing θ and the outgoing ϕ angles. The first factorization, after a reparametrization based on the half angle [Rus98], results in the product of 2D factors, stored as matrices. Let G be a $N_{\mathbf{w}} \times J$ matrix and F be a $J \times N_{\mathbf{w}_o}$ one. The G matrix multiplied by the F matrix is an approximation of Y. The second factorization of G, the view independent matrix, leads to the product of two 1D matrices, U and V. Using the non-negative matrix factorization (NMF) method [LS00] we always obtain matrices with positive values. The resulting L factors, where $L = J \times K$, show an intuitive approximation of a specific lobe of the original

BRDF.

$$f_r(\mathbf{w}_o,\mathbf{w}_i)\cos(\mathbf{w}_i) \approx \sum_{l=1}^{L} F_l'(\mathbf{w}_o)\,U_l'(\theta_\mathbf{w})\,V_l'(\phi_\mathbf{w}) = \sum_{l=1}^{L} T_l(\mathbf{w}_o,\theta_\mathbf{w},\phi_\mathbf{w})$$

We intended to use these factors as a PDF (Probabilistic Distribution Function), thus an upper limit should be calculated in order to normalize the factors. This sampling method was applied to the Cook-Torrance BRDF model [CT82], Poulin-Fournier cylindrical model [PF90], the anisotropic expression of Ward [War92], and also to acquired data from the public database of Matusik et al. [MPBM03]. Each BRDF must be efficiently and independently factorized making this method difficult to use for scenes containing many materials. Some functions will require many factors in order to be properly approximated. Thus, the user has to select the value of seven parameters manually: J, K, $(N_{\theta_{\mathbf{w}_o}} \times N_{\phi_{\mathbf{w}_o}})$, $(N_{\theta_\mathbf{w}} \times N_{\phi_\mathbf{w}})$ and which parametrization to use.

4.2.4. Directional and spatial variation approximation

The SVBRDF extends the BRDF to include spatial variation in reflectance making this function 6-dimensional. The work of Weistroffer et al. [WWHL07] intends to compactly represent data from spatially varying reflectance measurements, overcoming prior approaches by the fact of using a second level of indirection. The decomposition gives a sum of products of 2D (the blending weight) and 4D functions (the basis BRDF):

$$f_r(x,\mathbf{w}_o,\mathbf{w}_i) \approx \sum_{k=1}^{K} F_k(x) G_k(\mathbf{w}_o,\mathbf{w}_i) \tag{16}$$

The set G of primary basis is defined with respect to a secondary linear basis Υ:

$$f_r(x,\mathbf{w}_o,\mathbf{w}_i) \approx \sum_{k=1}^{K} F_k(x) \left[\sum_{l=1}^{L} \Gamma_{kl}\Upsilon_l(\mathbf{w}_o,\mathbf{w}_i)\right]$$

where Γ_{kl} is the weight vector that defines the primary linear basis.

One of the main virtues of this decomposition is the choice of the secondary basis. This allows selection of the more appropriate representation according to the nature and density of the available data. Υ could be spherical harmonics, wavelets (both discussed later in sections 4.4 and 4.5), acquired BRDFs or radial basis functions (RBF) [ZREB06]. The RBFs are designed to interpolate arbitrary smooth functions but they need to rely on a larger number of input samples. A comparison of RBF with the MERL isotropic BRDF dataset [MPBM03] concludes that the more restrictive basis of a dataset (the acquired one) is preferable, given that it is meant to represent reflectances.

4.2.5. Finding the required complexity

Mahajan et al. [MTR08] gave a theoretical and empirical analysis of the BRDF factorization. They answer an important question: how many terms do we need to represent a BRDF model accurately with a given parametrization? In some cases, as the Lawrence et al. factorization [LRR04], it is not just a single question. The user needs to decide which parametrization to use, the size of the initial data and of course, the number of factors. Mahajan et al. analyze the Phong BRDF starting from its spherical harmonic expansion, concluding the following statement: the numbers of terms needed are linear in the Phong exponent, and quadratic in the frequency content along the reflected or half-angle direction. With experimentation they found that this affirmation holds quite generally for many BRDFs from the MERL isotropic database [MPBM03].

4.3. Product of terms

The Homomorphic Factorization (HF) [MAA01] decomposes arbitrary BRDFs into the product of two or more factors of lower dimensionality and positive values. This method does not require tabulating the data into a matrix of the same resolution as the final representation. It deals with a sparse data matrix without resampling or interpolation. In this case, the decomposition is not a sum of terms but a product of positive factors of two dimensions. Those terms can be stored in texture maps after projection with function π.

$$f_r(\mathbf{w}_o,\mathbf{w}_i) \approx \prod_{j=1}^{J} t_j(\pi_j(\mathbf{w}_o,\mathbf{w}_i))$$

Then the authors use a logarithmic transformation of both sides of the equation. The resulting system is a linear data-fitting problem. An interesting aspect of this logarithmic transformation is the fact that minimizing the RMS error in logarithmic space is the same as minimizing the relative RMS error in the original space. This improves the solution as the perception of the human visual system is relative to the ratio of intensities and not to absolute quantities.

$$\log f_r(\mathbf{w}_o,\mathbf{w}_i) \approx \sum_{j=1}^{J} \log t_j(\pi_j(\mathbf{w}_o,\mathbf{w}_i))$$

The resolution of this system has to be reconverted to the original problem by exponentiating. Special care has to be taken with the logarithmic of zero-value reflectance data. Fixing J, we have a three-factor approximation of the BRDF:

$$f_r(\mathbf{w}_o,\mathbf{w}_i) \approx F(\mathbf{w}_o)\,G(\mathbf{h})\,F(\mathbf{w}_i) \tag{17}$$

$$\log f_r(\mathbf{w}_o,\mathbf{w}_i) \approx \log F(\mathbf{w}_o) + \log G(\mathbf{h}) + \log F(\mathbf{w}_i)$$

The numerical technique employed to find F and G is a linear system of constraints relating each sample of a BRDF to the corresponding texel locations in F and G. Additional equations are included in the linear system to set smoothing and weighting constraints to the solution. The homomorphic factorization expression Eq. (17) can be used with isotropic and anisotropic BRDFs. This representation is similar to SVD but avoids negative numbers and its flexibility allows to use any parametrization. Unfortunately McCool et

al. method does not allow for proof of optimality. A study and improvement of HF is given by [Col02] whose technique automatically selects the projection functions.

Another important BRDF approximation approach was presented based on the HF. In [LK02] the factorization considers the product of the BRDF and the lighting. Using a product function instead of a function, is in fact more complex, given that lighting uses global parametrization (and is defined over the sphere of directions) whereas the BRDF is defined with local parameters. This complexity is resolved by the use of isotropic BRDFs in arbitrary lighting conditions and a preprocessing step. With an isotopic BRDF not only do we have a reduction in the dimensionality (now 3D), but more importantly, the local coordinate frame $\mathbf{n}, \mathbf{t}, \mathbf{t} \times \mathbf{n}$ does not depend on the tangent vector.

$$L_r(\mathbf{w}_o) \approx \prod_{j=1}^{J} t_j(\pi_j(\mathbf{w}_o)) = t_1(\mathbf{n})\, t_2(\mathbf{r}_{\mathbf{w}_o})$$

The HF takes the logarithmic of both sides, yielding $\log L_r(\mathbf{w}_o) \approx \log t_1(\mathbf{n}) + \log t_2(\mathbf{r}_{\mathbf{w}_o})$. It is solved as a linear equation system with the Quasi-minimal residual (QMR) algorithm. The final solution comes from the exponentiation. As in [KM99] the approximation is based on textures, and the number of factors is fixed to $J = 2$, so only two textures are implemented. Using a mapping π, texture coordinates are converted to directions and vice versa.

4.4. Spherical harmonics

Spherical harmonics (SH) are the Fourier basis functions applied on the sphere, which is an upper set of the directional hemispherical domain of the BRDF. The use of a global reconstruction scheme such as the SH basis functions has been used in the literature of Computer Graphics. Some noteworthy papers are listed here:

- Cabral et al. [CMS87] have the idea of using the SH to derive isotropic BRDFs. They also give an expression of the lighting integral which was a simplified dot product. To reach that point, they make some simplifications: (1) it is assumed constant view direction, and (2) the SH coefficients are derived from a height field geometry, neither from an analytic evaluation of a BRDF model, nor from measured reflectance data.
- Westin et al. [WAT92] use spherical harmonics in the precomputational inference of a BRDF from geometric models. The view and lighting dependence on the BRDF is encoded in a matrix that stores the SH basis coefficients. In this case the evaluation of high-order basis functions is undertaken during rendering, and that implies low computational cost.
- Kautz et al. [KSS02] represent the four dimensional space of an arbitrary BRDF (any isotropic or anisotropic reflectance model) in a 2D table of spherical harmonics coefficients. Each entry represents the product of the incident light times the BRDF product function (the BRDF multiplied by the cosine of the normal with the incident direction). This representation is intended to account for low-frequency lighting and arbitrary BRDFs in real-time. This approach needs to compute the BRDF and the lighting coefficients for the Spherical Harmonic basis. The first one is precomputed by numerical integration. They first parametrize the BRDF product function by local view direction, which is represented by SH basis.

$$f_r(\mathbf{w}_o, \mathbf{w}_i)\cos(\mathbf{w}_i) = \sum_{i=1}^{N} c_i(\mathbf{w}_o) y_i(\mathbf{w}_i)$$

$$c_i(\mathbf{w}_o) = y_i(\mathbf{w}_i) \int f_r(\mathbf{w}_o, \mathbf{w}_i)\cos(\mathbf{w}_i)\, \max(0, z_{\mathbf{v}})\, d\sigma(\mathbf{w}_i)$$

The above integral —called the SH-projection— is also applied to the incoming lighting. By representing the lighting function as well as the SH basis, the lighting integral is reduced to a simple sum of dot products [CMS87]. To perform integration, we need to rotate the lighting into the BRDF's local frame with a single computation in SH space. The rotated coefficients of c_i are computed via linear transformation. Moreover, for low-frequency lighting, few components ($N = 25$) are required and the computation of this integral and its projection into SH basis can be performed on-the-fly. If both lighting and material contain higher frequencies, then the number of coefficients (understood as resolution or quality of the approximation) should be incremented to achieve good results.

4.5. Wavelets

If we have decided to represent the BRDF in tabular form, it can be helpful to build on the model of wavelets given that this approach is widely employed in other fields of science for data compression (in particular 2D images). The wavelet transform $\mathcal{W}$ is a linear operator that can encode a general function f in a process named the analysis of the function f:

$$\mathcal{W} : (f : A \to B) \to \mathcal{T}(f)$$

$$\mathcal{T}(\alpha f + \beta g) = \alpha \mathcal{T}(f) + \beta \mathcal{T}(g)$$

The analysis consists of projecting the function at different resolutions or scales $l \in \mathbb{N}$. The mother basis function $\Psi_l = \psi_l^m : A \to B$ is the wavelet itself. Commonly the Haar basis is used as mother function. The scaling functions $\Phi_{l+1} = \phi_{l+1}^k : A \to B$ are used to derive the wavelets at resolution l. The wavelet transform is a recursive decomposition of the function f at different levels or resolutions from the coarse level $l = 0$ to the finest $l = n$.

$$f = \sum_k a_0^k \phi_0^k + \sum_{l=0}^{n} \sum_m d_l^m \psi_l^m$$

where a_l^k and d_l^m are the projection coefficients. The discrete wavelet transformation produces the same number of coefficients as the original samples, but those whose value is zero or below a threshold are discarded and not stored, thus achieving compression. The synthesis or reconstruction of f uses a similar recursive procedure.

The more outstanding qualities of this representation are:

- generality: it can represent any function,
- compression: it can achieve important compression rates most notably with large datasets,
- trade-off between accuracy/space easily controlled,
- multiresolution: reconstruction at different levels of accuracy,
- reconstruction from the piece-wise function is effectively computed in $O(\log N)$ where N is the number of BRDF samples,
- simple error metrics,
- denoising: the wavelet smoothly interpolates the original data,
- it preserves high and low frequency features during the decomposition step, and therefore typical reflectance peaks of a glossy BRDF are well preserved,
- there are sampling procedures to use the approximated BRDF in a Monte-Carlo algorithm for Global Illumination.

Some of the most representative works related to BRDF compression using wavelets are commented upon in the following subsections.

4.5.1. Spherical Wavelet Decomposition

The more common wavelet functions are on $\mathbb{R}$ but there are also Spherical Wavelets [SS95]. This basis constructs a regular subdivision of an octahedron or a tetrahedron (for $\mathcal{S}^2$ or Ω spaces) which is independent of the spherical parametrization of the incoming and outgoing directions. After the subdivision of the domain in triangles, the BRDF is approximated by a piece-wise constant function on the triangle at a specified level of subdivision. The value of the function —a single value $f_r(\mathbf{w}_o, \mathbf{w}_i)$ or the whole spectrum response $f_r(\mathbf{w}_o, \mathbf{w}_i, \lambda)$ in [CBP02]— is stored in the triangle in the direction of the triangle centre. The scaling and wavelet functions are an area extension of the Haar basis functions, and they are known as Bio-Haar basis [SS95].

4.5.2. Multidimensional Wavelet Decomposition

Lalonde and Fournier [LF97] presented an approximated BRDF model based on the projection of the BRDF onto a 4D wavelet basis. This dimensionality comes from the product of four 1D basis that are computed following the standard decomposition —the non-standard approach would need to use the product of multidimensional basis— after a reparametrization of $\Omega \times \Omega$ domain into $\mathbb{R}^4$. More specifically $(\theta, \phi) \in \Omega$ is mapped to $(\kappa, \gamma) \in \mathbb{R}^2$.

The BRDF is decomposed as follows:

$$\begin{aligned} f_r(\mathbf{w}_o, \mathbf{w}_i) &= f_r(\kappa_{\mathbf{w}_o}, \gamma_{\mathbf{w}_o}, \kappa_{\mathbf{w}_i}, \gamma_{\mathbf{w}_i}) \\ &= \sum_g \sum_h \sum_j \sum_k B_g(\kappa_{\mathbf{w}_o}) B_h(\gamma_{\mathbf{w}_o}) B_j(\kappa_{\mathbf{w}_i}) B_k(\gamma_{\mathbf{w}_i}) \end{aligned}$$

The general bases are defined as:

$$B_n(x) = \begin{cases} \Phi(x) \text{ if } n > 0 \text{ with } l, m \geq 0 \\ 2^{l/2} \Upsilon(l^{-l} x - m) \text{ if } n = 2^l + m \end{cases}$$

where Ψ is the mother wavelet, Φ is the smoothing function and l is the level in the wavelet subspace.

Favorably, this representation includes the cosine term for the projected area. One minor drawback of this representation comes from the parametrization, which filled corner zones with zeros and they are stored even though they give no information. If there are so many wavelet coefficients as original data points, we have no compression at all. For this reason, the selection of a convenient data structure is important. Lalonde and Fournier recommend the use of a hash table or a *wavelet coefficient tree* that stores only the coefficients indexed by the wavelet basis selector, however introducing a pointer set cost.

To reconstruct the BRDF at a given set of directions $d = (\kappa_{\mathbf{w}_o}, \gamma_{\mathbf{w}_o}, \kappa_{\mathbf{w}_i}, \gamma_{\mathbf{w}_i})$, each coefficient for which B_n is non-zero needs to be consulted. Resulting time complexity is $O(w^4 l^4)$ where w is the wavelet width.

4.5.3. Generic Wavelet Decomposition

This is a wavelet representation for a reflectance function dependent on the wavelength of incoming light —also known as spectral BRDF— and thus with five dimensional complexity. Furthermore this representation is also suitable for path tracing. It appears in [CPB03, CBP, CPB06] and is based on the separation of the BRDF into two components: a spectral and a geometrical component. The function f_r is then $\Omega \times \Omega \times \mathbb{R} \to \mathbb{R}$. Fixing $\mathbf{w}_o$, we have $f_r(\mathbf{w}_i, \lambda) : \Omega \times \mathbb{R} \to \mathbb{R}$ which is equivalent to $f_r(\mathbf{w}_i) : \Omega \to (f_r(\lambda) : \mathbb{R} \to \mathbb{R})$. This transformation is key for the generic wavelet transform because now we have a spherical function $f_r(\mathbf{w}_i)$ whose elements are one-dimensional real $f_r(\lambda)$ functions. The authors apply multiple simple transformations. Firstly a spherical wavelet changes the spherical signal and gives as a result the wavelet and scaling coefficient vectors. Secondly a one-dimensional transform is applied to vector data resulting in the final coefficients. The second transformation is more effective and compresses more than the spherical domain because spectral values tend to be smoother. The combination of the spherical transformation and the spectral one provide the full transformation of the spectral reflectance distribution function, obtaining a compression rate of more than 90%.

As we have already pointed out, coefficients with zero or a value below a threshold are ignored, leaving a sparse set of data which has to be stored efficiently. In this case the recommended data structure [CPB03] is the *sparse array*, a double-linked list of strips. The strip node stores a bit array of valid/invalid positions together with the array data. An optimal number of strips is crucial for the storage saving of this structure. In [CPB06] a two-threshold scheme is recommended, one for the spherical transformation and other for the spectral transformed coefficients. The fact that the BRDF diffuse component yields more compressed results even by using different thresholds for each of the BRDF components, makes them to develop a formula for adaptively computing the threshold. This local value ensures a relative uniform compression.

In [CPB06,CBP07] a general Generic Wavelet Transform (GWT) framework is intended to be used with acquired spectral reflectance data in a real-time per-pixel rendering system. The coefficients of the 4D wavelet transformation are stored in 3D texture maps and their processing is performed on the GPU using a fragment shader. The full 4D decomposition is done in two steps. First they transform the sphere domain $\mathcal{S}^2$ in $\mathbb{R}^2$ with a given mapping. Then, the spherical wavelet transform [SS95] is applied twice: the 2D wavelet transformation for the incoming and the outgoing hemispheres of directions. Directions correspond with triangles and wavelets, and each triangle data is stored on a high-resolution texture. The number and textures that the fragment shader uses depend on a resolution parameter that is chosen automatically for the BRDF reconstruction. This level-of-detail reconstruction allows for optimal antialiasing of surfaces at a distance from the observer.

5. Sampling the BRDF

The way of distributing random samples is known as the probability distribution function (PDF). In Monte Carlo algorithms for Global Illumination the generation of random sample directions (to estimate the reflected radiance) is a frequent task and should be performed as quickly as possible. In order to render realistic images, we have to use realistic material models, although few of them provide a method for sampling with the desired PDF and properties (that is, proportional to the BRDF and fast). Some BRDFs [TS67,CT82] are impractical in rendering systems for this reason, tough some approximations could be used as the ones presented in the following sections.

A good definition of the PDF is the key to the effectiveness of the final MC estimator. It is preferable to generate more samples where the function has higher values —that is what *importance sampling* (IS) does— because with uniform sampling we will have under-sample regions in which high values of the function occur, leading to visible error in the image. It is also important to ensure that a region with non-null BRDF values would have a non-null probability to be sampled. Importance sampling gives better solutions when the PDF is chosen closer to the integrand but it is not easy to find for a wide-range of BRDF models. A possible solution to use the BRDF for IS is to have a mathematical framework that forces plausible BRDFs. Edwards et al [EBJ*06] create an empirical BRDF from the transformation of halfway vectors into different domains assuming its integral can be a PDF. This constraint enforces energy conservation. Thus the unit radius disk is a good domain to specify BRDF properties such as specular and retro-reflection.

5.1. Monte-Carlo based BRDF sampling

If we consider any algorithm which generates random direction vectors (or samples) in the hemisphere Ω, the distribution of those samples is determined by a probability measure, which obviously depends directly on that algorithm. We will symbolize probability as P. For any region $R \subseteq \Omega$, the real value $P(R)$ is the probability for the random vector to be in region R.

Measure P usually depends on a vector $\mathbf{v}$ in the hemisphere. For clarity, we will express this dependence explicitly in the notation by writing $P_\mathbf{v}$ for the particular probability measure associated to any vector $\mathbf{v} \in \Omega$. Usually $P_\mathbf{v}(\Omega) = 1$, although for some algorithms, samples are produced in the hemisphere under the surface. For those cases, measure P is defined on the whole sphere $\mathcal{S}^2$, with $P(\mathcal{S}^2) = 1$.

The probability distribution function (PDF) is the density of $P_\mathbf{u}$ with respect to solid angle measure in the hemisphere, that is for any $\mathbf{u},\mathbf{v} \in \Omega$, the real value $p_\mathbf{v}(\mathbf{u})$ is defined as $dP_\mathbf{v}(\mathbf{u})/d\sigma(\mathbf{u})$. When a PDF p is used to sample a BRDF f_r, it must hold this condition:

$$f_r(\mathbf{u},\mathbf{v}) > 0 \implies p_\mathbf{u}(\mathbf{v}) \geq 0 \text{ and } p_\mathbf{v}(\mathbf{u}) \geq 0$$

When using a PDF $p_\mathbf{u}$ for sampling a BRDF f_r, we can obtain an estimation of the reflected radiance at $\mathbf{u}$ by using a weighted average of the estimated radiance values for each sample direction $\{\mathbf{v}_1,\ldots,\mathbf{v}_n\}$:

$$L_r(\mathbf{u}) = \frac{1}{n}\sum_{i=1}^{n} w_i L'_r(\mathbf{v}_i) \quad \text{where} \quad w_i = \frac{f_r(\mathbf{u},\mathbf{v}_i)\cos(\mathbf{v}_i)}{p_\mathbf{u}(\mathbf{v}_i)}$$

The values $L_r(\mathbf{v}_i)$ can be approximated by using the same method recursively, as it is done in raw path-tracing [Kaj86], or by using a different method, as in the method proposed by Ward et al. [WRC88] (where pre-computed radiance estimates are used) or in final gathering for Photon-mapping [Jen01] (where radiance estimation for secondary rays are obtained from the photon-map).

In the following sections we review particular sampling strategies for particular BRDF models. In all of the cases, the problem is to find a particular map M with the property described above, and which can be efficiently evaluated.

5.2. Direct Sampling

Usually the PDF is chosen to mimic a specific model, and this situation is known as *direct sampling*.

Ideal Diffuse Case. A perfect diffuse BRDF reflects energy equally distributed in Ω. This simple BRDF ($f_r = k_d/\pi$, where $0 \leq k_d \leq 1$) has an associated PDF $p_\mathbf{u}(\mathbf{v}) = \cos(\mathbf{v})/\pi$ which is exactly proportional to the BRDF times the cosine term and also independent of $\mathbf{u}$. To get a random vector $\mathbf{v}$ distributed according the PDF, compute:

$$(\theta_\mathbf{v},\phi_\mathbf{v}) = \left(\arccos(\sqrt{\xi_1}), 2\pi\xi_2\right)$$

where ξ_1 and ξ_2 are two independent uniformly distributed random variables with values in $[0,1)$. From this point we will use ξ notation with this meaning.

Ideal Specular Case. The PDF is a Dirac-delta function $p_\mathbf{u}(\mathbf{v}) = \eth_\mathbf{u}(\mathbf{v})$, and thus a sample distributed according to this PDF is $\mathbf{r_u}$ with probability 1, and any other values

have probability 0. As a consequence, generating random directions consists simply of producing $\mathbf{r_u}$ for a given $\mathbf{u}$.

Lobe Distribution Sampling. BRDFs based on cosine-lobes [Pho75, Bli77, Lew94, LFTG97, War92] have an associated algorithm for sampling. The single-lobe BRDF is defined as:

$$f_r(\mathbf{u},\mathbf{v}) = C(n)\,(\mathbf{v}\cdot\mathbf{r_u})^n$$

where $n \geq 0$ is a parameter, and $C(n)$ is a normalization factor which usually depends on n. This ensures these BRDFs have an energy conservation property.
For this BRDF class, the directional-hemispherical reflectivity can be written as:

$$\rho_n(\mathbf{u}) = C(n) N_2(\mathbf{r_u}, n)$$

where, for any vector $\mathbf{a}$, $N_2(\mathbf{a},n)$ is defined as:

$$N_2(\mathbf{a},n) \stackrel{\text{def}}{=} \int_\Omega (\mathbf{v}\cdot\mathbf{a})^n\,(\mathbf{v}\cdot\mathbf{n})\,d\sigma(\mathbf{v})$$

which is called a *double axis moment*. Arvo [Arv95b] provided an analytical expression for N_2. It is easy to show that $N_2(\mathbf{a},n) \leq N_2(\mathbf{n},n)$, as $N_2(\mathbf{n},n) = 2\pi/(n+2)$ (thus it can be easily evaluated). A usual option for $C(n)$ is $1/N_2(\mathbf{n},n)$ ensuring energy conservation and yielding a simple BRDF model which can be evaluated very fast:

$$f_r(\mathbf{u},\mathbf{v}) = \frac{n+2}{2\pi}\,(\mathbf{v}\cdot\mathbf{r_u})^n$$

A related normalized PDF can be defined as:

$$p_\mathbf{u}(\mathbf{v}) = \frac{1}{N_1(\mathbf{r_u},n)}\,(\mathbf{v}\cdot\mathbf{r_u})^n$$

where N_1 ensures normalization and is defined as:

$$N_1(\mathbf{a},n) \stackrel{\text{def}}{=} \int_\Omega (\mathbf{v}\cdot\mathbf{a})^n\,d\sigma(\mathbf{v})$$

This is called a *single axis moment* and, as for N_2, it is possible to give analytical expressions for N_1. In order to obtain samples distributed according to this PDF, we first obtain a random vector $\mathbf{v}$ whose spherical coordinates are:

$$(\theta,\phi) = \left(\arccos\left(\xi_1^{\frac{1}{n+1}}\right), 2\pi\xi_2\right)$$

$\mathbf{r_v} = (\sin(\theta)\cos(\phi), \sin(\theta)\sin(\phi), \cos(\theta))$ is computed, and after this, we rotate $\mathbf{r_v}$ by using R, where R is the rotation which converts $\mathbf{n}$ into $\mathbf{r_u}$, that is $\mathbf{r_u} = R(\mathbf{n})$. The resulting sample is then $\mathbf{s} = R(\mathbf{r_v})$. Note that this yields unit vectors outside Ω (with a probability smaller than $1/2$), and in these cases we must reject those samples and try to produce a new one until a valid one is obtained. The exponent n is a parameter of this sampling method.

Half-angle based The reflectance models [Bli77, War92, KSK01] calculate vector $\mathbf{h}$ as $(\theta_\mathbf{h},\phi_\mathbf{h}) = (\sqrt[n+1]{\xi_1}, 2\pi\xi_2)$. Reflected vector $\mathbf{v}$ is returned with a probability of

$$p_\mathbf{u}(\mathbf{v}) = \frac{n+1}{2\pi}\,\frac{\cos^n(\theta_\mathbf{h})}{4\,(\mathbf{v}\cdot\mathbf{h})}$$

The above formulation includes the correct proportion between the measures:

$$p_\mathbf{u}(\mathbf{v}) = p_\mathbf{h}(\mathbf{v})\left\|\frac{d\sigma(\mathbf{h})}{d\sigma(\mathbf{u})}\right\| \tag{18}$$

$$\begin{aligned}\frac{d\sigma(\mathbf{h})}{d\sigma(\mathbf{u})} &= \frac{\sin(\theta_\mathbf{h})\,d\theta_\mathbf{h}\,d\phi_\mathbf{h}}{\sin(\theta_\mathbf{v})\,d\theta_\mathbf{v}\,d\phi_\mathbf{v}} = \frac{\sin(\theta_\mathbf{h})\,d\theta_\mathbf{h}\,d\phi_\mathbf{h}}{\sin(2\theta_\mathbf{h})\,2d\theta_\mathbf{h}\,d\phi_\mathbf{h}} \\ &= \frac{\sin(\theta_\mathbf{h})}{4\cos(\theta_\mathbf{h})\sin(\theta_\mathbf{h})} = \frac{1}{4\cos(\theta_\mathbf{h})} \\ &= \frac{1}{4\,(\mathbf{v}\cdot\mathbf{h})} = \frac{1}{4\,(\mathbf{u}\cdot\mathbf{h})}\end{aligned}$$

5.3. General Sampling

General sampling methods deal with arbitrary reflectance models and measured data. This will permit the use of complex reflectance distribution functions in Global Illumination applications and in real-time rendering. Many papers have been published for this topic mostly based on sampling by inversion procedure, or on the rejection sampling technique.

- Lalonde and Fournier [LF97] use numerical inversion of the BRDF for sampling purposes using the wavelet representation. Samples are generated directly from the wavelet data structure.
- The Homomorphic Factorization [MAA01] decomposes arbitrary BRDFs or measured data into the product of two or more factors which are stored as texture maps. Fixing the direction $\mathbf{w}_o$, either $G(\mathbf{h})$ or $F(\mathbf{w}_i)$ (see section 4.3) can be used as a PDF to generate randomly outgoing sampled directions. If samples are generated according to the half-vector some corrections should be done to the final distribution, as we have already pointed out in Eq. (18).
- The MERL BRDF database [†] is an approximate representation of a hundred isotropic surfaces, with a resolution of 90 x 180 x 90. Matusik et al. [MPBM03] developed a generic sampling algorithm for these measured data. The procedure computes a 2D cumulative distribution function (CDF) over incident directions according to the spherical parametrization of the hemisphere. This requires dense sampling along all variables (even more storage than the BRDF itself). Given that a single isotropic BRDF is 33 MB, this sampling scheme is not compact.
- The Spherical Wavelet BRDF representation has the advantage of a *wavelet sampling* technique [CPB03]. An alternative tree structure independent of the representation stores the BRDF $f_r^\lambda = \int_\lambda f_r(\mathbf{w}_o,\mathbf{w}_i,\lambda)d\lambda$ as the monochromatic version with the cosine term included.
  To randomly sample a direction $\mathbf{s}$, first they choose a piece of the representation, a triangle, using its CDF. Thus, a triangle projected onto the hemisphere on level j, T_j^k, is then uniformly sampled. The fact that each triangle value at level j is the average of its children values at level $j+1$

[†] Available on line at: <http://www.merl.com/brdf/>

enables a recursive search procedure making the algorithm's complexity dependent on the number of triangles. The conditional probability is computed as the probability of selecting a triangle times the probability of the uniformly sampled value. To reduce the bias in their sampling method [CBP07] the selection and descent of a child triangle use random permutation of the children instead of a sequential search. The complexity of this algorithm is logarithmic in the number of spherical triangles.

- Wavelet Importance Sampling (WIS) [CJAMJ05] generates values that are proportional to the product of two N-dimensional functions, the BRDF and the lighting, given their representation using Haar-based wavelets. The product is a new wavelet defined by the product coefficients of both wavelet representations. The algorithm starts from a coarse level of representation towards the fine level of the wavelet tree, warping points according to $f_r \cdot L_i$ by following a probability defined by the scalar coefficients of the child nodes. It is not an exact technique for sampling because the representation of both functions, reflectance and lighting, comes from sparse levels of detail.
- The factorization of analytical and measured reflectance models [LRR04] includes a sampling procedure. The non-negative matrix factorization (NMF), ensures that the factors are always positive, and facilitates the use of normalized factors as a CDF for numerical inversion sampling. First the algorithm selects the lobe l that contributes most energy for the current view $\mathbf{u}$, according to the F matrix (see section 4.2.3). The CDF for this sampling is recomputed when the outgoing direction changes. Next, the hemisphere is sampled according to the selected lobe l by sequential generation of the elevation and the azimuthal angles using the precomputed CDF for U_l and V_l. The density function for the generated outgoing direction is:

$$p_{\mathbf{u}}(\mathbf{v}) \;=\; q(\mathbf{w}) \left\| \frac{d\sigma(\mathbf{w})}{d\sigma(\mathbf{v})} \right\| \;=\; \frac{1}{4(\mathbf{v}\cdot\mathbf{h})} \sum_{l}^{L} \frac{T_l(\mathbf{u},\theta_{\mathbf{w}},\phi_{\mathbf{w}})}{\sum_j^L F_j(\mathbf{u})}$$

  where $\mathbf{w}$ is the parametrization vector, L is the number of lobes, and $\mathbf{u},\mathbf{v}$ usually stand for $\mathbf{w}_o$ and $\mathbf{w}_i$ respectively.
- The Cascade CDF method [LRR05] is an adaptive technique oriented to sampling acquired reflectance data. It is based on sampling by inversion of the CDF, and instead of uniformly distributing the samples, it uses a second and equivalent distribution which is compact. The method starts with a N-dimensional PDF and divides it into the product of a 1D marginal distribution $\tilde{p}$ and a set of 1D conditional distributions.

$$\tilde{p}(x) \;=\; \int_{-\infty}^{\infty} p(x,y)\, dy$$

$$p(y|x_i) \;=\; \frac{1}{x_i - x_{i-1}} \int_{x_{i-1}}^{x_i} \frac{p(x',y)}{\tilde{p}(x')}\, dx'$$

  Compression is carried out using the *Douglas-Peucker* greedy algorithm [Ros97] which approximates a curve (in this case the CDF) employing an optimal number of segments. Applying the aforementioned to BRDF sampling the authors recommend starting from an initial dense set of data. The required processing time and memory to compute the adaptive representation may vary with each BRDF. We applied this technique to the MERL BRDF database to test the compression of data. Some of the results are shown in table 2. With a resolution $(\theta_{\mathbf{u}} \times \phi_{\mathbf{u}} \times \theta_{\mathbf{h}} \times \phi_{\mathbf{h}})$ of $32 \times 16 \times 256 \times 32$, each uniformly-sampled CDF occupies 33 MB. We can see that average compression rate is 98%, mostly in non-specular reflectance data.
- In [MULG08] an importance sampling algorithm for arbitrary BRDFs and measured data is presented. This method has the benefit of optimal rejection sampling, in the sense of bounded trials. It has few and intuitive parameters that could be set as constants. A scene with many reflectance models can be rendered using the same algorithm's configuration for each BRDF instance, avoiding user guidance in terms of adjusting parameters for each BRDF. The core data of this approach is a set of hierarchical quadtree structures: one for each $(f_r, \mathbf{w}_o)$ pair. Each precomputed quadtree subdivides the disc domain $[-1,+1]^2$, adaptively in a recursive way. Samples on the disc will follow a distribution which is exactly proportional to the BRDF times the cosine term. The subdivision criteria is a parameter of the method which ensures that rejection sampling on leaf nodes can be done with an *a priori* bounded number of average trials. This algorithm gives favourable results when used with a set of common and complex BRDF models and also with MERL isotropic BRDF database, even in the same scene. This PDF can be integrated with other techniques such as Resampling Importance Sampling (RIS) [TCE05].

To compare direct and general sampling we have used the Dragon model from Stanford University[‡]. The reflectance function used in this scene corresponds to Oren-Nayar [ON94] with a roughness value of 0.83, and an instance of Strauss BRDF [Str90] mostly smooth for floor and wall, respectively. The dragon itself has a Lafortune BRDF [LW94] with exponent $n = 46$. The rendering is in figure 7. With this mixture of BRDFs, we can compare the Disc sampling method with uniform sampling, cosine lobe in Ω, and Lawrence et al. [LRR04] factored representation. For the cosine lobe and the factored BRDF we adjusted the parametrization manually to fit the shape of each BRDF instance. Note that the cosine lobe technique is suited for lobe-based BRDFs and no others. From left to right, the sampling time are: 9.749, 29.06, 24.539 and 42.632 seconds respectively. With only 100 samples, Disc PDF [MULG08] gives less noise than the others, with no need for manual adjusting.

6. Conclusions

Our main objective is to divulge common understanding of a wide range reflectance models. For this reason, we have

[‡] The Stanford 3D Scanning Repository is on-line at <http://graphics.stanford.edu/data/3Dscanrep/>

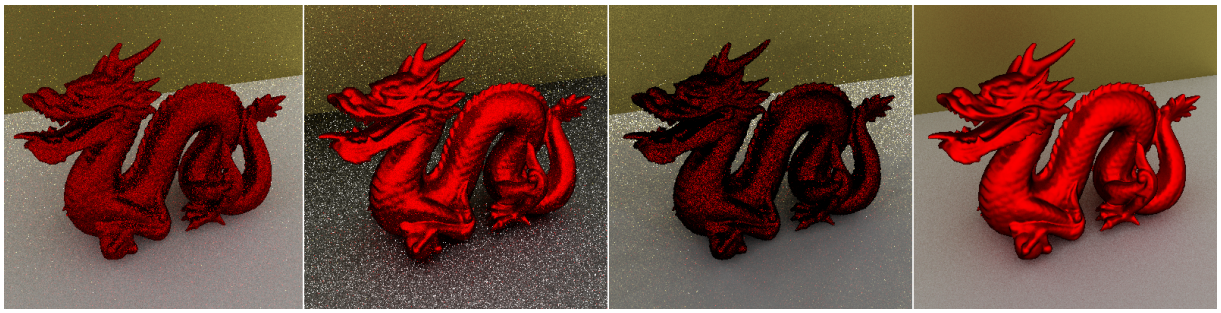

Figure 7: *From left to right, images corresponding to the Uniform PDF, adjusted cosine-lobe strategy in Ω, the Factored representation of the BRDF and the Disc PDF. With only 100 samples, Disc PDF algorithm performs better, as the scene has three different instances of BRDFs.*

MERL BRDFs	Time (sec)	Mem. (KB)	Reduc.
alum-bronze	572.13	998.15	97.05%
alumina-oxide	577.4	174.75	99.48%
aluminium	568.31	1156.5	96.58%
aventurnine	562.68	331.65	99.02%
beige-fabric	559.53	187.66	99.44%
black-fabric	579.51	265.13	99.22%
black-obsidian	580.54	802.2	97.63%
black-oxidized-steel	575.38	761.45	97.75%
black-phenolic	577.38	901.96	97.33%
black-soft-plastic	562.24	799.8	97.63%
blue-acrylic	576.79	382.53	98.87%
blue-fabric	578.26	351.58	98.96%
blue-metallic-paint2	572.29	1038.0	96.93%
blue-metallic-paint	575.35	1110.05	96.72%
nickel	567.49	1023.62	96.97%
red-plastic	586.5	275.83	99.18%
teflon	561.78	184.51	99.45%
violet-acrylic	578.69	826.69	97.55%
white-marble	565.71	247.79	99.27%
yellow-paint	566.06	143.47	99.58%

Table 2: *Requirements of Cascade CDF method when the original CDF is compressed and adaptively sampled.*

presented the fundamentals of the reflectance function, its characteristics and the environment in which it is used. With the intention of be a complement of information on how to choose, use or even implement a specific model we have overview a set of papers that cover a wide range of the full bibliography. For each BRDF we briefly expose its formulation and applicability, and we have covered issues of interest in representations and sampling methods.

We also have reviewed important contributions about the possible representations of the BRDF and how to sample according to it, giving a survey of techniques to *Importance Sample* the BRDF function in a Monte-Carlo rendering system.

Acknowledgement

The authors have been partially supported by the Spanish Research Program under project TIN2004-07672-C03-02 and the Andalusian Research Program under project P08-TIC-03717.

References

[APS00] ASHIKHMIN M., PREMOŽE S., SHIRLEY P.: A microfacet-based BRDF generator. In *SIGGRAPH '00: Proceedings of the 27th annual conference on Computer graphics and interactive techniques* (New York, USA, 2000), ACM Press/Addison-Wesley Publishing Co., pp. 65–74. 10, 14

[Arv95a] ARVO J.: *Analytic Methods for Simulated Light Transport*. PhD thesis, Yale University, December 1995. 2

[Arv95b] ARVO J.: Applications of irradiance tensors to the simulation of non-lambertian phenomena. In *SIGGRAPH '95: Proceedings of the 22nd annual Conference on Computer Graphics and Interactive Techniques* (1995), ACM Press, pp. 335–342. 20

[AS00] ASHIKHMIN M., SHIRLEY P.: An anisotropic phong BRDF model. *Journal on Graphics Tools 5*, 2 (2000), 25–32. 9

[ATS94] ARVO J., TORRANCE K., SMITS B.: A framework for the analysis of error in global illumination algorithms. In *Proceedings of the 21st annual conference on Computer graphics and interactive techniques* (New York, NY, USA, 1994), SIGGRAPH '94, ACM, pp. 75–84. 3

[Bli77] BLINN J. F.: Models of light reflection for computer synthesized pictures. In *SIGGRAPH '77: Proceedings of the 4th annual conference on Computer graphics and interactive techniques* (New York, NY, USA, 1977), ACM Press, pp. 192–198. 11, 20

[BS63] BECKMANN P., SPIZZICHINO A.: *The Scattering*

of Electromagnetic Waves from Rough Surfaces. Pergamon Press, New York, 1963. Reprinted in 1987 by Artech House Publishers, Norwood, Massachusetts. 6, 7

[CBP] CLAUSTRES L., BOUCHER Y., PAULIN M.: Wavelet projection for modelling of acquired spectral BRDF. *Optical Engineering. SPIE - The International Society for Optical Engineering 43*, 10, 2327–2339. 18

[CBP02] CLAUSTRES L., BOUCHER Y., PAULIN M.: Spectral BRDF modeling using wavelets. Szu H. H., Buss J. R., (Eds.), vol. 4738, SPIE, pp. 33–43. 14, 18

[CBP07] CLAUSTRES L., BARTHE L., PAULIN M.: Wavelet encoding of BRDFs for real-time rendering. In *Proceedings of Graphics Interface 2007* (New York, NY, USA, 2007), GI '07, ACM, pp. 169–176. 19, 21

[CJAMJ05] CLARBERG P., JAROSZ W., AKENINE-MÖLLER T., JENSEN H. W.: Wavelet importance sampling: efficiently evaluating products of complex functions. *ACM Trans. Graph. 24*, 3 (2005), 1166–1175. 21

[CMS87] CABRAL B., MAX N., SPRINGMEYER R.: Bidirectional reflection functions from surface bump maps. In *SIGGRAPH '87: Proceedings of the 14th annual conference on Computer graphics and interactive techniques* (New York, NY, USA, 1987), ACM, pp. 273–281. 14, 17

[Col02] COLE F. H.: *Automatic BRDF Factorization*. PhD thesis, Harvard College, Cambridge, Massachusetts, April 2002. 17

[CP85] CLARKE F., PARRY D.: Helmholtz reciprocity: Its validity and application to reflectometry. *Lighting Research and Technology 1*, 17 (1985), 1–11. 3

[CPB03] CLAUSTRES L., PAULIN M., BOUCHER Y.: BRDF measurement modelling using wavelets for efficient path tracing. *Computer Graphics Forum. European Association for Computer Graphics and Blackwell Publishing 22*, 4 (December 2003), 701–716. 14, 18, 20

[CPB06] CLAUSTRES L., PAULIN M., BOUCHER Y.: A wavelet-based framework for acquired radiometric quantity representation and accurate physical rendering. *Visual Computer. Springer Berlin Heidelberg 22* (April 2006), 221–237. 14, 18, 19

[CT82] COOK R., TORRANCE K.: A reflectance model for computer graphics. *ACM Computer Graphics (SIGGRAPH'81 Proceedings) 1*, 1 (1982), 7–24. 7, 16, 19

[Dan01] DANA K. J.: BRDF/BTF measurement device. In *Proceedings of Eighth IEEE International Conference on Computer Vision* (2001), vol. 2, pp. 460–466. 14

[DBB06] DUTRÉ P., BALA K., BEKAERT P.: *Advanced global illumination*. Ak Peters Series. AK Peters (CRC Press), 2006. 2, 3

[DGNK99] DANA K. J., GINNEKIN B. V., NAYAR S. K., KOENDERINK J. J.: Reflectances and texture of real-world surfaces. 1–34. 5, 14

[Dür06] DÜR A.: An improved normalization for the ward reflectance model. *Journal of Graphics, GPU, and Game Tools 11*, 1 (2006), 51–59. 12

[EBJ*06] EDWARDS D., BOULOS S., JOHNSON J., SHIRLEY P., ASHIKHMIN M., STARK M., WYMAN C.: The halfway vector disk for BRDF modeling. *ACM Trans. Graph. 25*, 1 (2006), 1–18. 19

[Fou95] FOURNIER A.: Separating reflection functions for linear radiosity. In *Proceedings of the Eurographics Rendering Workshop 1995* (June 1995), Eurographics, pp. 296–305. 14, 15

[GA97] GERMER T., ASMAIL C.: A goniometric optical scatter instrument for bidirectional reflectance distribution function measurements with out-of-plane and polarimetry capabilities. In *Scattering and Surface Roughness. Proc. SPIE 3141* (1997), Z.-H. Gu and A.A. Maradudin, Editors, pp. 220–231. 4, 14

[GA99] GERMER T., ASMAIL C.: Goniometric optical scatter instrument for out-of-plane ellipsometry measurements. *Review of Scientific Instruments 70* (September 1999), 3688–3695. 4

[GH03] GRANIER X., HEIDRICH W.: A simple layered rgb BRDF model. *Graph. Models 65*, 4 (2003), 171–184. 10

[Gla94] GLASSNER A. S.: *Principles of Digital Image Synthesis*, vol. 2. Morgan Kaufmann Publishers Inc., San Francisco, CA, USA, 1994. 2

[GMD10] GEISLER-MORODER D., DÜR. A.: A new ward BRDF model with bounded albedo. *Computer Graphics Forum 29* (June 2010), 1391–1398. 12

[GMW81] GILL P., MURRAY W., WRIGHT M.: *Practical Optimization*. Academic Press, 1981. 14

[Hec02] HECHT E.: *Optics*. Addison-Wesley, 2002. 2

[Hel25] HELMHOLTZ H.: Treatise on physiological optics. *Nature 1*, 17 (1925), 358–382. 3

[HHP*92] HE X. D., HEYNEN P. O., PHILLIPS R. L., TORRANCE K. E., SALESIN D. H., GREENBERG D. P.: A fast and accurate light reflection model. *SIGGRAPH Computer Graphics 26*, 2 (1992), 253–254. 9

[HLW06] HONGSONG LI SING-CHOONG FOO K. E. T., WESTIN S. H.: Automated three-axis gonioreflectometer for computer graphics applications. *Optical Engineering*, 45 (2006), 043605. 4

[HTSG91] HE X., TORRANCE K., SILLION F., GREENBERG D.: A comprehensive physical model for light reflection. In *SIGGRAPH '91: Proceedings of the 18th annual conference on Computer graphics and interactive techniques* (New York, NY, USA, July 1991), no. 4, ACM Press, pp. 175–186. 8, 9

[Jen01] JENSEN H. W.: *Realistic Image Synthesis Using Photon Mapping*. AK Peters, 2001. 19

[Kaj85] KAJIYA J. T.: Anisotropic reflectance models. In

Computers Graphics, ACM Siggraph'85 Conference Proceedings (July 1985), no. 4, pp. 15–21. 8

[Kaj86] KAJIYA J. T.: The rendering equation. In *SIGGRAPH '86: Proceedings of the 13th annual conference on Computer graphics and interactive techniques* (New York, NY, USA, 1986), ACM Press, pp. 143–150. 19

[KC08] KURT M., CINSDIKICI M. G.: Representing BRDFs using SOMs and MANs. *SIGGRAPH Comput Graph 42*, 3 (2008), 1–18. 5

[KM99] KAUTZ J., MCCOOL M. D.: Interactive rendering with arbitrary BRDFs using separable approximations. In *Proceedings of the 10th Eurographics Workshop on Rendering* (June 1999), Eurographics, pp. 281–.292. 14, 15, 17

[KSK01] KELEMEN C., SZIRMAY-KALOS L.: A microfacet based coupled specular-matte BRDF model with importance sampling. In *Eurographics Conference. Short presentations* (2001), pp. 25–34. 20

[KSS02] KAUTZ J., SLOAN P.-P., SNYDER J.: Fast, arbitrary BRDF shading for low-frequency lighting using spherical harmonics. In *EGRW '02: Proceedings of the 13th Eurographics workshop on Rendering* (Aire-la-Ville, Switzerland, Switzerland, 2002), Eurographics Association, pp. 291–296. 13, 17

[KvDS96] KOENDERINK J. J., VAN DOORN A. J., STAVRIDI M.: Bidirectional reflection distribution function expressed in terms of surface scattering modes. In *ECCV '96: Proceedings of the 4th European Conference on Computer Vision-Volume II* (London, UK, 1996), Springer-Verlag, pp. 28–39. 14, 15

[Lew94] LEWIS R. R.: Making shaders more physically plausible. *Computer Graphics Forum 13*, 2 (1994), 109–120. 11, 20

[LF97] LALONDE P., FOURNIER A.: A wavelet representation of reflectance functions. *IEEE Transactions on Visualization and Computer Graphics 3*, 4 (1997), 329–336. 14, 18, 20

[LFTG97] LAFORTUNE E. P., FOO S.-C., TORRANCE K. E., GREENBERG D. P.: Non-linear approximation of reflectance functions. In *SIGGRAPH '97: Proceedings of the 24th annual conference on Computer graphics and interactive techniques* (New York, NY, USA, 1997), ACM Press/Addison-Wesley Publishing Co., pp. 117–126. 11, 13, 14, 20

[LK02] LATTAZ L., KOLB A.: Homomorphic factorization of BRDF-based lighting computation. In *SIGGRAPH '02: Proceedings of the 29th annual conference on Computer graphics and interactive techniques* (New York, NY, USA, 2002), ACM, pp. 509–516. 14, 17

[LM01] LEUNG T., MALIK J.: Representing and recognizing the visual appearance of materials using three-dimensional textons. *Int. J. Comput. Vision 43*, 1 (2001), 29–44. 15

[LRR04] LAWRENCE J., RUSINKIEWICZ S., RAMAMOORTHI R.: Efficient BRDF importance sampling using a factored representation. In *Proceedings of the 2004 SIGGRAPH Conference* (August 2004), no. 3, ACM Transaction of Graphics, pp. 496–505. 14, 15, 16, 21

[LRR05] LAWRENCE J., RUSINKIEWICZ S., RAMAMOORTHI R.: Adaptive numerical cumulative distribution functions for efficient importance sampling. In *Eurographics Symposium on Rendering* (2005), pp. 11–20. 21

[LS00] LEE D., SEUNG H.: Algorithms for non-negative matrix factorization. In *NIPS* (2000), pp. 556–562. 15

[LW94] LAFORTUNE E. P., WILLEMS Y. D.: *Using the Modified Phong Reflectance Model for Physically Based Rendering*. Tech. Rep. Report CW197, Department of Computer Science, K.U.Leuven, Leuven, Belgium, November 1994. 21

[MAA01] MCCOOL M. D., ANG J., AHMAD A.: Homomorphic factorization of BRDFs for high-performance rendering. In *SIGGRAPH 2001, Computer Graphics Proceedings* (2001), Fiume E., (Ed.), ACM Press / ACM SIGGRAPH, pp. 185–194. 14, 16, 20

[MBW*73] MAXWELL J. R., BEARD J., WEINER S., LADD D., LADD S.: *Bidirectional reflectance model validation and utilization*. Tech. rep., AFAL–TR–73–303, Environmental Research Institute of Michigan (ERIM), October 1973. 7

[MH84] MILLER G. S., HOFFMAN C. R.: Illumination and reflection maps: Simulated objects in simulated and real environments. In *Course Notes from Advances Computer Graphics Animation SIGGRAPH 84*. ACM Press, July 1984. 8

[Min41] MINNAERT M.: The reciprocity principle in lunar photometry. *Astrophysical Journal*, 3 (1941), 403–410. 10

[MPBM03] MATUSIK W., PFISTER H., BRAND M., MCMILLAN L.: A data-driven reflectance model. *ACM Trans. Graph. 22*, 3 (2003), 759–769. 5, 14, 16, 20

[MTR08] MAHAJAN D., TSENG Y.-T., RAMAMOORTHI R.: An analysis of the in-out BRDF factorization for view-dependent relighting. *Comput. Graph. Forum 27*, 4 (2008), 1137–1145. 16

[MULG08] MONTES R., UREÑA C., LASTRA M., GARCIA R.: Generic BRDF sampling: A sampling method for global illumination. In *GRAPP 2008 Proceedings of the Third International Conference on Computer Graphics Theory and Applications* (Funchal, Madeira, Portugal, January 2008), pp. 191–198. 21

[MWM*98] MEISTER G., WIEMKER R., MONNO R., SPITZER H., STRAHLER A.: Investigation on the torrance-sparrow specular BRDF model. In *Geoscience and Remote Sensing Symposium Proceedings* (1998), IEEE International, pp. 2095–2097. 6, 12

[NDM05] NGAN A., DURAND F., MATUSIK W.: Experimental analysis of BRDF models. In *Proceedings of Eurographics Symposium on Rendering* (2005), Eurographics Association, pp. 117–226. 5, 9, 14

[NN96] NEUMANN L., NEUMANN A.: *A New Class of BRDF Models with Fast Importance Sampling*. Tech. Rep. TR-186-2-96-24, December 1996. 11

[NNSK99] NEUMANN L., NEUMANN A., SZIRMAY-KALOS L.: Compact metallic reflectance models. In *Computer Graphics Forum (Eurographics '99)* (1999), Brunet P., Scopigno R., (Eds.), vol. 18(3), The Eurographics Association and Blackwell Publishers, pp. 161–172. 12

[NRH*92] NICODEMUS F. E., RICHMOND J. C., HSIA J. J., GINSBERG I. W., LIMPERIS T.: Radiometry. Jones and Bartlett Publishers, Inc., , USA, 1992, ch. Geometrical considerations and nomenclature for reflectance, pp. 94–145. 1, 2

[OKBG08] OZTURK A., KURT M., BILGILI A., GUNGOR C.: Linear approximation of bidirectional reflectance distribution functions. *Computers & Graphics 32*, 2 (2008), 149–158. 14

[ON94] OREN M., NAYAR S.: Generalization of lambert's reflectance model. In *SIGGRAPH '94: Proceedings of the 21st annual conference on Computer graphics and interactive techniques* (New York, NY, USA, 1994), ACM Press, pp. 239–246. 9, 21

[ON95] OREN M., NAYAR S.: Visual appearance of matte surfaces. *Science 267*, 5201 (February 1995), 1153–1156. 9

[PF90] POULIN P., FOURNIER A.: A model for anisotropic reflection. In *SIGGRAPH '90: Proceedings of the 17th annual conference on Computer graphics and interactive techniques* (New York, NY, USA, August 1990), no. 4, ACM Press, pp. 273–282. 8, 16

[PH10] PHARR M., HUMPHREYS G.: *Physically Based Rendering: From Theory to Implementation*. Morgan Kaufmann. Elsevier Science & Technology, 2010. 2

[Pho75] PHONG B.-T.: Illumination for computer generated pictures. In *Computers Graphics, ACM Siggraph'75 Conference Proceedings* (New York, NY, USA, June 1975), no. 6, ACM Press, pp. 311–317. 10, 13, 20

[Ros97] ROSIN P. L.: Techniques for assessing polygonal approximations of curves. In *IEEE Transactions on Pattern Analysis and Machine Intelligence* (1997), no. 6, pp. 659–666. 21

[Rus98] RUSINKIEWICZ S.: A new change of variables for efficient BRDF representation. In *Nineth Eurographics Workshop on Rendering* (June 1998), pp. 11–23. 4, 15

[Sch93] SCHLICK C.: A customizable reflectance model for everyday rendering. In *Fourth Eurographics Workshop on Rendering, Eurographics'93* (June 1993), no. 93, pp. 73–84. 12

[Sch94a] SCHLICK C.: A fast alternative to phong's specular model. In *Graphics Gems*. Eds Paul Heckbert, Academic Press, 1994, pp. 363–366. 9, 10, 13

[Sch94b] SCHLICK C.: An inexpensive BRDF model for physically-based rendering. In *Proc. Eurographics'94, Computer Graphics Forum* (1994), no. 3, pp. 233–246. 6, 10, 12

[Shi90] SHIRLEY P.: *Physically Based Lighting Calculations for Computer Graphics*. Phd. dissertation, University of Illinois at Urbana Champaign, December 1990. 1

[Shi96] SHIRLEY P.: Monte carlo methods for rendering. In *ACM SIGGRAPH '96 Course Notes - Global Illumination in Architecture and Entertainment*. 1996, pp. 1–26. 5

[SHSL97] SHIRLEY P., HU H., SMITS B., LAFORTUNE E.: A partitioners' assessment of light reflection models. In *Pacific Graphics 97 conference proceedings* (1997), pp. 40–49. 9, 12

[SS95] SCHRÖDER P., SWELDENS W.: Spherical wavelets: efficiently representing functions on the sphere. In *SIGGRAPH '95: Proceedings of the 22nd annual conference on Computer graphics and interactive techniques* (New York, NY, USA, 1995), ACM, pp. 161–172. 18, 19

[Str90] STRAUSS P. S.: A realistic lighting model for computer animators. *IEEE Computer Graphics Applications 10*, 6 (1990), 56–64. 11, 21

[TCE05] TALBOT J. F., CLINE D., EGBERT P. K.: Importance resampling for global illumination. In *Rendering Techniques 2005 (Eurographics Symposium on Rendering)* (June 2005), pp. 139–146. 21

[TS66] TORRANCE K., SPARROW E.: Off-specular peaks in the directional distribution of reflected thermal radiation. In *Journal of Heat Transfer* (May 1966), pp. 223–230. 6, 7

[TS67] TORRANCE K., SPARROW E.: Theory for off-specular reflection. In *Journal of the Optical Society of America* (September 1967), no. 9. 6, 7, 19

[Vea97] VEACH E.: *Robust Monte Carlo methods for light transport simulation*. Ph.d. dissertation, Stanford University, 1997. 3

[Wal05] WALTER B.: *Notes on the ward BRDF*. Tech. Rep. PCG-05-06, Cornell Program of Computer Graphics, 4 2005. 12

[War92] WARD G. J.: Measuring and modeling anisotropic reflection. In *Computers Graphics, ACM Siggraph'92 Conference Proceedings* (July 1992), no. 4, pp. 265–272. 4, 12, 13, 14, 16, 20

[WAT92] WESTIN S. H., ARVO J. R., TORRANCE K. E.: Predicting reflectance functions from complex surfaces. In *Computers Graphics, ACM Siggraph'92 Conference Proceedings* (New York, NY, USA, July 1992), no. 2, ACM Press, pp. 255–264. 9, 13, 14, 15, 17

[WM02] WESTLUND H. B., MEYER G. W.: A BRDF database employing the beard-maxwell reflection model. *Graphics Interface 2002 proceedings Calgary Alberta 2729 May 2002* (2002), 189. 7

[WRC88] WARD G., RUBINSTEIN F., CLEAR R.: A ray tracing solution for diffuse interreflection. In *Computers Graphics, ACM Siggraph'88 Conference Proceedings* (August 1988), no. 4, pp. 85–92. 19

[WWHL07] WEISTROFFER R. P., WALCOTT K. R., HUMPHREYS G., LAWRENCE J.: Efficient basis decomposition for scattered reflectance data. In *EGSR07: Proceedings of the Eurographics Symposium on Rendering* (Grenoble, France, June 2007), pp. 207–218. 16

[ZREB06] ZICKLER T., RAMAMOORTHI R., ENRIQUE S., BELHUMEUR P. N.: Reflectance sharing: Predicting appearance from a sparse set of images of a known shape. *IEEE Transactions on Pattern Analysis and Machine Intelligence 28*, 8 (2006), 1287–1302. 16